AD_____

Award Number: DAMD17-01-1-0382

TITLE: The Role of Fps in Tumor-Associated Angiogenesis

PRINCIPAL INVESTIGATOR: Waheed Sangrar, Ph.D.

CONTRACTING ORGANIZATION: Queen's University
Kingston, Ontario
Canada   K7L 3N6

REPORT DATE: July 2003

TYPE OF REPORT: Annual Summary

PREPARED FOR: U.S. Army Medical Research and Materiel Command
Fort Detrick, Maryland   21702-5012

DISTRIBUTION STATEMENT: Approved for Public Release;
Distribution Unlimited

The views, opinions and/or findings contained in this report are
those of the author(s) and should not be construed as an official
Department of the Army position, policy or decision unless so
designated by other documentation.

20031212 079

REPORT DOCUMENTATION PAGE

Form Approved
OMB No. 074-0188

Public reporting burden for this collection of information is estimated to average 1 hour per response, including the time for reviewing instructions, searching existing data sources, gathering and maintaining the data needed, and completing and reviewing this collection of information. Send comments regarding this burden estimate or any other aspect of this collection of information, including suggestions for reducing this burden to Washington Headquarters Services, Directorate for Information Operations and Reports, 1215 Jefferson Davis Highway, Suite 1204, Arlington, VA 22202-4302, and to the Office of Management and Budget, Paperwork Reduction Project (0704-0188), Washington, DC 20503

1. AGENCY USE ONLY (Leave blank)	2. REPORT DATE July 2003	3. REPORT TYPE AND DATES COVERED Annual Summary (1 Jul 2002 - 30 Jun 2003)

4. TITLE AND SUBTITLE
The Role of Fps in Tumor-Associated Angiogenesis

5. FUNDING NUMBERS
DAMD17-01-1-0382

6. AUTHOR(S)
Waheed Sangrar, Ph.D.

7. PERFORMING ORGANIZATION NAME(S) AND ADDRESS(ES)
Queen's University
Kingston, Ontario
Canada K7L 3N6

E-Mail: ws4@post.queensu.ca

8. PERFORMING ORGANIZATION REPORT NUMBER

9. SPONSORING / MONITORING AGENCY NAME(S) AND ADDRESS(ES)
U.S. Army Medical Research and Materiel Command
Fort Detrick, Maryland 21702-5012

10. SPONSORING / MONITORING AGENCY REPORT NUMBER

11. SUPPLEMENTARY NOTES
Original contains color plates: All DTIC reproductions will be in black and white.

12a. DISTRIBUTION / AVAILABILITY STATEMENT
Approved for Public Release; Distribution Unlimited

12b. DISTRIBUTION CODE

13. ABSTRACT (Maximum 200 Words)

The tyrosine kinase Fps has been implicated in angiogenesis. Expression of activated Fps (MFps) causes hyper-vascularity in mice (fps^{MF} mice) suggesting that Fps may regulate angiogenesis. Studies have shown that the magnitude of vascularity is elevated 1.7-fold and is highly-disorganized and tortuous in nature. Stimulation of endothelial cells (EC) isolated from these mice has shown that MFps, but not Fps is activated in response to PDGF and VEGF. This suggests that MFps mediates hyper-sensitization of EC to these growth factors, an abnormality which may underlie the proangiogenic phenotype in these mice. In other studies we have shown early tumor onset in the context of loss-of-function Fps genetic backgrounds suggesting that Fps may behave as a tumor suppressor. Thus, Fps may be a suitable target for the development of anti-tumorigenic and anti-angiogenic therapeutics. Lastly, fps^{MF} mice may have a DIC-like phenotype. This was suggested by hemostatic defects and by an array of phenotypic features characteristic of disorders associated with vascular hyperplasia. This is an important finding, since DIC occurs as a lethal complication in advanced cancers, including those of the breast.

14. SUBJECT TERMS
Transgenic mice, breast cancer, tumorigenesis, angiogenesis, tyrosine kinase, cytokines, oncogenes, hemangioma, metastases

15. NUMBER OF PAGES
88

16. PRICE CODE

17. SECURITY CLASSIFICATION OF REPORT Unclassified	18. SECURITY CLASSIFICATION OF THIS PAGE Unclassified	19. SECURITY CLASSIFICATION OF ABSTRACT Unclassified	20. LIMITATION OF ABSTRACT Unlimited

NSN 7540-01-280-5500

Standard Form 298 (Rev. 2-89)
Prescribed by ANSI Std. Z39-18
298-102

Table of Contents

TRAINING REPORT: 2nd ANNUAL SUMMARY

INTRODUCTION

The ability of tumor cells to execute angiogenic programs is critical for their progression to malignant and metastatic states [reviewed in [1,2]]. Transgenic expression of an activated form of the cytoplasmic tyrosine kinase Fps (MFps) gave rise to mice (fps^{MF}) with pronounced hyper-vascularity[3]. This suggested that Fps may directly or indirectly regulate angiogenic mechanisms. Our work to date has utilized molecular, cellular and physiological approaches to elucidate how Fps may affect angiogenesis. These approaches have in part, led to new insights which suggest that Fps may have tumor suppressor-like properties. These approaches have also revealed defects in blood coagulation and fibrinolysis, which is not surprising given that the hemostatic system has been proposed to be a regulator of angiogenesis[4]. More specifically, we observed that fps^{MF} mice may potentially have a disseminated intravascular coagulation (DIC)-like pathology. This is an important finding since DIC is a potentially lethal complication of advanced cancers[5,6]. Thus, fps^{MF} mice may represent an important new model for the study of this pathology.

Our work is still ongoing along the proposed Statement of Work. A primary question this ongoing work will address pertains to whether Fps directly regulates angiogenesis by affecting endothelial sprouting, or whether it indirectly regulates this process through other related processes such as coagulation and inflammation.

PROGRESS ASSOCIATED WITH STATEMENT OF WORK

Objective #1: Assessment of the effect of *fps* and *fer* allelic variant on tumorigenesis in a mouse breast tumor model.

a. Breeding pairs designed to produce offspring that generate tumors in fps^0, fps^{KR} and fps^{MF} genetic backgrounds were generated in the 1st year. Generation of breeding pairs which give rise to tumorigenic fps^{KR}/fps^{DR} and fer^{DR} mice was, and is still delayed due to time constraints and resources.

b. Monitoring of tumor diameter in mice with fps^0 and fps^{KR} genetic background is now fully complete. We have observed and confirmed statistically, an early onset of tumorigenesis in loss-of-function *fps* genetic backgrounds which suggests that Fps may have tumor-suppressor-like properties. On the other hand, we have been unable to generate sufficient number of tumorigenic mice with a fps^{MF} genetic background. We suspect that embryos of this genotype are dying *in utero* since there is significant evidence for decreased viability of offspring from hemizygous fps^{MF} x *wild-type* (*wt*) breeding pairs.

c. Lung metastases was in the process of being monitored in tumorigenic mice harboring fps^0 and fps^{KR} alleles. We have completed this assessment and were unable to observe significant differences in the number of metastasized nodules between *wt* and *fps* loss-of-function mice suggesting that Fps does not play a role in metastases [7].

d. In the 1st year we had quantified the vascular area in fps^{MF} mice using intra-vital microscopy on cremaster muscle. These results indicated a 1.7-fold increase in vascular area in these mice and as well, revealed that their vascular system is highly disorganized and tortuous in nature. These and other related results are summarized in a manuscript entitled: "Vascular defects in gain-of-function *fps/fes* transgenic mice correlate with PDGF- and VEGF-induced activation of mutant Fps/Fes kinase in endothelial cells".[8]

Objective #2: Assessment of the endothelial cell (EC) immortalizing ability of *fps* relative to the known EC immortalizing/transforming agent polyoma middle T(PymT).

a. pMSCV-based retroviruses encoding PymT, *fps*, fps^{KR} and fps^{MF} were successfully generated in the 1st year.

4

b. Primary cells from day 12 yolk-sacs of *wt* mice were transduced with the retroviruses generated in Objective #2a and transduced cells were isolated using puromycin drug selection. We had problems quantifying EC composition in the 1st year and have made several repeated attempts since, however we have not been successful. Our predominant difficulty is likely technical in that we have experienced problems with cell viability after isolation, infection and selection. The original isolation of C166 EC cells from these mice was a stochastic phenomenon, and we anticipate that a significantly large number of attempts would have to be made to quantify the EC immortalizing ability of *fps* relative to PymT. The latter considerations, coupled with difficulties in establishing this technique, has lowered the priority of this Objective. As a result, significant progress has not been made along this line.

Objective #3: Generation of EC lines from different *fps* genetic backgrounds for *in vitro* studies.
a. pMSCV-based retroviruses encoding PymT and SV40-T were successfully generated in the 1st year.
b. We had made several attempts at generating endothelial cells from aortic and lung explants in the 1st year. However, difficulties were encountered generating sufficient numbers of EC populations using explant and flow-cytometry-based cell sorting methods. As a result, there has been a delay in completing this Objective. We were considering, and are now currently developing a magnetic cell-sorting approach for generating EC lines.

Objective #4: Assessment of the role of Fps in angiogenesis *in vitro*.
a. In the 1st year we established methods enabling visualization of neovascularization from fibrin-immobilized aorta and yolk-sacs.
b. We did not observe differences in the vascularity of yolk-sacs between *wt* and *fps*^{MF} mice suggesting that the hyper-vascular defect occurs subsequent to vasculogenesis, potentially during the remodeling phases of angiogenesis. Preliminary work performed in the 1st year did not indicate any difference in neovascularization between *wt* and *fps*^{MF} mice in yolk-sac explants. We have since decided to examine neovascularization from aortic explants. Work on this Objective has been temporarily postponed, but we intend to complete this Objective as it will be important to assess whether the hyper-vascular phenotype in *fps*^{MF} mice is due to a direct effect of MFps on neovascularization, or whether it is a secondary effect of other processes affected by MFps transgenic expression. Completing this objective will help to address this question.
c. Assessment of angiogenesis using perforated polycarbonate chambers implanted in mice has not been performed, as we are awaiting the results from Objective 4b.
d. Completion of Objective 3b is required for testing the ability of immortalized ECs to form tubules in fibrin-gels.
e. C166 cell lines expressing myc-epitope-tagged forms of kinase-inactive Fps (FpsKR), myristoylated Fps (MFps) and Fps were generated in the 1st year.
f. We have done preliminary experiments testing the ability of cell lines generated in Objective 4e to form tubules in fibrin gels. We are currently optimizing this assay by titrating the number of cells immobilized in fibrin gels. This optimization was found to be necessary for comparison of the tubule-formation capacity of the different cell lines.

Objective #5: Assessment of coagulation and fibrinolytic parameters in *fps*^{MF} mice.
a. Standardized PT and APTT assay have been completed this year. We have also previously determined coagulation parameters using platelet aggregation and tail bleeding assays (see key accomplishments below).
b. *In vitro* clot lysis assays have been completed.

Objective #6: Examination of proteolytic expression profiles of cell lines expressing Fps.

a. In the 1st year we examined matrix metalloproteinase (MMP) expression profiles of primary macrophages and observed enhanced gelatinase activity of a band migrating at 90 kDa in *fps*^{MF} mice. However, since then, we have been unable to observe this consistently, suggesting that MMP expression is normal in macrophages isolated from *fps*^{MF} mice.

b. Examination of uPA and MMP-2/-9 activity of cell cultures of immortalized ECs will be completed pending achievement of Objective #3. uPA and MMP-2/-9 expression levels of the cell lines generated in Objective 4e will also be tested and is already in progress.

Objective #7: Elucidation of the role of Fps in signaling pathways potentiated by VEGF, bFGF and thrombin.

a. Activation of (M)Fps downstream of the thrombin receptor was observed in C166 cells. This activation was a late and inconsistent event suggesting that (M)Fps is activated by a cytokine/growth factor autocrine mechanism triggered by thrombin. Earlier studies showed that C166 cells are insensitive to basic-fibroblast growth factor (bFGF) and vascular endothelial growth factor (VEGF). However since then, we have been able to confirm subtle activation of MFps but not Fps in response to VEGF[8]. Also in C166 cells, we have confirmed that MFps, but not Fps is strongly activated in response to platelet-derived growth factor (PDGF).[8] These results suggest that MFps abnormally sensitizes endothelial cells to both VEGF and PDGF.[8]

b. Signaling studies in immortalized ECs in the different Fps genetic backgrounds will begin upon completion of Objective #3. The results of Objective 7a show that MFps is responsive to VEGF and PDGF, but *wt* Fps is not. The effects of these agonists on immortalized *wt* and *fps*^{MF} ECs will be explored to further elucidate the mechanistic basis of the angiogenic defect in *fps*^{MF} mice.

KEY RESEARCH ACCOMPLISHMENTS

- Early onset of tumorigenesis has been confirmed in *fps*^{0} and *fps*^{KR} genetic backgrounds suggesting a potential tumor suppressor-like role for this kinase. Since *fps*^{MF} displayed a proangiogenic phenotype, we had originally expected that *fps* loss-of-function mice would impact negatively on the angiogenic process and hence inhibit tumorigenesis. The reported observation is both unexpected and exciting since it opens up possibilities of designing anti-tumorigenic therapeutics based on directly or indirectly enhancing Fps activity. Interestingly, mutational analyses of the tyrosine kinome in colorectal cancers detected 4 Fps/Fes tumor-specific single-mutation variants in the kinase domain[9]. We have recently generated Fps/Fes constructs which incorporate kinase-domain mutations and preliminary results intriguingly indicate that 3 of 4 mutations negatively influence kinase activity while the other has no effect. These results concur with the *in vivo* evidence suggesting that Fps may have tumor suppressor-like properties. We are still in the process of confirming the kinase activity assays and we intend to publish these results within the next year.[7]

- The work from Objective 1d, 4d and 7a has formed the basis of a manuscript recently submitted to the American Journal of Pathology. This work is summarized in the manuscript entitled: "Vascular defects in gain-of-function *fps/fes* transgenic mice correlate with PDGF- and VEGF-induced activation of mutant Fps/Fes kinase in endothelial cells"[8] (See Reportable Outcomes/Appended Document).

- Fps has been previously implicated in myelopoiesis, the process which gives rise to granulocytes, and monocytes. Macrophages are important modulators of angiogenesis and we have therefore hypothesized that Fps may modulate angiogenesis indirectly through alteration of macrophage function. Hematological analysis of *fps*^{MF} mice had revealed increased output of cells of the myeloid lineage, and bone-marrow methyl-cell assays suggested that myelopoiesis is significantly

elevated in these mice. Whether elevated myelopoiesis is a contributing factor to the hyper-vascular phenotype however, is still unclear. These results are essentially an outgrowth of Objective #4, which was concerned with assessing the role of Fps in angiogenesis. They have formed the basis of a manuscript submitted to Experimental Hematology that is entitled: "The *fps/fes* proto-oncogene regulates hematopoietic lineage output"[10] (See Reportable Outcomes/Appended Document).

- Understanding the general physiological phenotype of *fps*[MF] mice will be essential for uncovering the basis of the proangiogenic phenotype of these mice. To date, we have observed an array of physiological anomalies in these mice which have led to several new observations related to the angiogenic phenotype of *fps*[MF] mice. In particular, assessment of the coagulation and fibrinolysis parameters proposed in Objective 5a and 5b led to the development of two manuscripts that have recently been submitted for publication or are under revision (See Reportable Outcomes). These manuscripts are concerned with secondary effects associated with hyper-vascularity. They present evidence for a DIC-like state in these mice as suggested by phenotypical features characteristic of Kasabach Merritt Syndrome and as well, by various coagulation and fibrinolytic parameters unique to these mice. Thus, *fps*[MF] mice may constitute an important model for DIC and hence would comprise an invaluable tool for the study of this secondary phenomenon that manifests as a lethal complication in advanced tumors, including those of the breast[5,6].

REPORTABLE OUTCOMES
Promotion
The research stemming from this award has been a significant factor in my promotion to Assistant Professor (adjunct) level at Queen's University (Appended Document).

Abstracts
1) **W. Sangrar**, R.A. Zirngibl, J. Mewburn, Y.A. Senis, C. Chapler, D.H.Lee and P.A. Greer. A murine transgenic line expressing a myristylated form of Fps/Fes is characterized by disorganized hyper-vascular patterning and peripheral blood defects. *Blood* **98**, 31a. *43rd Annual A.S.H. Meeting.* Orlando, Florida, 7th-12th December, 2001.
2). **W. Sangrar**, J. Mewburn, Y. Senis, R.A. Zirngibl, Man Y. Tse, S.G. Vincent, M.L. Scott, S.C. Pang, D.H. Lee, J.T. Fisher and P.A. Greer. Mice expressing gain-of-function Fps/Fes are characterized by vascular malformation, aberrant levels of circulating blood cells and potential defects in endothelial, platelet and macrophage function. *Breast Cancer Era of Hope Meeting*, Orlando, Florida, September 25th-28th, 2002.

Manuscripts *submitted* for publication
1) **W. Sangrar**, Y.A. Senis, Y. Gao, M. Richardson, J. Samis and P.A. Greer. Bleeding defects and thrombocytopenia in transgenic mice expressing an activated mutant Fps/Fes non-receptor protein-tyrosine kinase is associated with disseminated intravascular coagulation. *Manuscript in revisions for Blood (May 2003).*
2) **W. Sangrar**, R.A. Zirngibl, M.Y. Tse, S.C. Pang, D.H. Lee and P.A. Greer. Gain-of-function *fps* transgenic mice: A model for Kasabach Merritt Syndrome. *Manuscript submitted to Journal of Pathology (July. 2003)*
3) **W. Sangrar**, Y. Gao, R.A Zirngibl, M.L. Scott, P.A Greer. The *fps/fes* proto-oncogene regulates hematopoietic lineage output *Manuscript submitted to Experimental Hematology. (June 2003).*
4) **W. Sangrar**, J. Mewburn, S.G. Vincent, M.Y. Tse, S.C. Pang, J.T. Fisher, and P.A. Greer. Vascular defects in gain-of-function *fps/fes* transgenic mice correlate with PDGF- and VEGF-induced activation of mutant Fps/Fes kinase in endothelial cells. *Manuscript submitted to American Journal of Pathology (July 2003).*

Manuscripts *in preparation* for publication

1). **W. Sangrar**, Y. Gao, R.A. Zirngibl, W. Muller, P.A. Greer.: Early mammary tumor onset in mice harboring kinase inactivating and null mutations of the *fps/fes* proto-oncogene. Manuscript in preparation (75% Complete: Proposed Submission Date: December, 2003).

CONCLUSIONS

The results reported here are significant in that they suggest a potential role for Fps in tumorigenesis as a tumor suppressor. This could have important future implications for the design of anti-tumorigenic therapeutics that are based on indirectly or directly elevating the activity of Fps.

The proangiogenic phenotype in *fps^{MF}* mice underscores an important role for this kinase in regulating mechanisms of angiogenesis. At this point we are unsure whether this kinase directly regulates angiogenesis through effects on the endothelium or whether it indirectly regulates this process through effects on other physiological functions such as coagulation (a process that is highly inter-related to angiogenesis[4]). In either case, these mice constitute an important tool for studying mechanisms which directly or indirectly contribute to angiogenesis; this will be important for ultimately understanding how tumors induce neoangiogenesis.

DIC is a secondary complication that often arises in advanced stages of cancer and can have lethal consequences[5,6]. *fps^{MF}* mice may constitute an important new model for studying the pathogenesis of DIC and for testing therapeutics which combat this pathology.

REFERENCES

1. Kerbel RS: Tumor angiogenesis: past, present and the near future. Carcinogenesis 2000, 21:505-515
2. Risau W: Mechanisms of angiogenesis. Nature 1997, 386:671-674
3. Greer P, Haigh J, Mbamalu G, Khoo W, Bernstein A, Pawson T: The Fps/Fes protein-tyrosine kinase promotes angiogenesis in transgenic mice. Mol Cell Biol 1994, 14:6755-6763.
4. Browder T, Folkman J, Pirie-Shepherd S: The hemostatic system as a regulator of angiogenesis. J Biol Chem 2000, 275:1521-1524
5. Sallah S, Wan JY, Nguyen NP, Hanrahan LR, Sigounas G: Disseminated intravascular coagulation in solid tumors: clinical and pathologic study. Thromb Haemost 2001, 86:828-833
6. Pasquini E, Gianni L, Aitini E, Nicolini M, Fattori PP, Cavazzini G, Desiderio F, Monti F, Forghieri ME, Ravaioli A: Acute disseminated intravascular coagulation syndrome in cancer patients. Oncology 1995, 52:505-508
7. Sangrar W, Zirngibl R, Greer PA: Early mammary tumour onset in mice harboring kinase inactivating and null mutations of the fps/fes proto-oncogene. Manuscript in preparation (75% Complete: Proposed Submission Date: December, 2003) 2003
8. Sangrar W, Mewburn J, Tse M, Vincent S, Pang S, Fisher J, Greer P: Vascular defects in gain-of-function fps/fes transgenic mice correlate with PDGF- and VEGF-induced activation of mutant Fps/Fes kinase in endothelial cells. Submitted to the American Journal of Pathology (June 2003)
9. Bardelli A, Parsons DW, Silliman N, Ptak J, Szabo S, Saha S, Markowitz S, Willson JK, Parmigiani G, Kinzler KW, Vogelstein B, Velculescu VE: Mutational analysis of the tyrosine kinome in colorectal cancers. Science 2003, 300:949
10. Sangrar W, Gao Y, Zirngibl RA, Scott ML, Greer PA: The fps/fes proto-oncogene regulates hematopoietic lineage output. Manuscript submitted to Experimental Hematology (July 2003)

LIST OF APPENDED ITEMS

1) Letter of Promotion.

2) W. Sangrar, J. Mewburn, S.G. Vincent, M.Y. Tse, S.C. Pang, J.T. Fisher, and P.A. Greer. Vascular defects in gain-of-function *fps/fes* transgenic mice correlate with PDGF- and VEGF-induced activation of mutant Fps/Fes kinase in endothelial cells. *Manuscript submitted to American Journal of Pathology (July 2003).*

3) W. Sangrar, Y. Gao, R.A Zirngibl, M.L. Scott, P.A Greer. The *fps/fes* proto-oncogene regulates hematopoietic lineage output *Manuscript submitted to Experimental Hematology. (June 2003).*

Queen's
UNIVERSITY

May 5, 2003

John T. Fisher, PhD
Associate Dean, Academic Affairs

FACULTY OF HEALTH SCIENCES

Dr. Waheed Sangrar
Rm A305, Botterell
Queen's University

Botterell Hall, Room 234
Queen's University
Kingston, Ontario, Canada K7L 3N6
Tel 613 533-6000 ext 77575
Fax 613 533-6884

Dear Dr. Sangrar:

On behalf of Principal William Leggett, Vice-Principal (Academic) Suzanne Fortier and Dean David Walker and on the recommendation of Dr. Iain Young, Head of Department, I am pleased to offer you appointment to the Adjunct (Group 1) academic staff in the Department of Pathology and Molecular Medicine at the rank of Assistant Professor for the term May 1, 2003 to June 30, 2004. Adjunct appointments may be renewed on an annual basis at the beginning of the academic year, in July, subsequent to recommendation by the Head of your Department. A copy of the University's Senate Statement on Adjunct Academic Staff and Academic Assistants as last revised June 23, 1994 is enclosed for your information.

While the appointment carries with it no university salary, it will afford you access to the libraries and certain other university facilities. To find out how to receive the required staff card, upon taking up your appointment please contact Mrs. Heather Miller in the Faculty of Health Sciences Office at 533-6000 extension 75963.

I would like to take this opportunity to welcome you as a member of the adjunct academic staff and I trust that you will find your association with Queen's a pleasant and academically rewarding one.

Yours truly,

Encl.

c.c.   Dr. I.D. Young, Head, Department of Pathology and Molecular Medicine
       Dr. D.M.C. Walker, Dean, Faculty of Health Sciences
       Human Resources

[hm]

Vascular defects in gain-of-function *fps/fes* transgenic mice correlate with PDGF- and VEGF-induced activation of mutant Fps/Fes kinase in endothelial cells

Running Title: Vascular defects in gain-of-function *fps/fes* transgenic mice.

Waheed Sangrar[1], Jeff Mewburn[1], Sandra G. Vincent[2], Man Y. Tse[3], Stephen C. Pang[3], John T. Fisher[2] and Peter A. Greer[1,4*].

[1]Division of Cancer Biology and Genetics, Queen's University Cancer Research Institute

[2]Department of Physiology and Medicine, Queen's University

[3]Department of Anatomy and Cell Biology, Queen's University

[4]Department of Pathology, Queen's University

*To whom correspondence should be addressed: Peter A. Greer, Division of Cancer Biology and Genetics, Queen's University Cancer Research Institute, Botterell Hall, Room A309, Kingston, Ontario, K7L 3N6, Canada. Tel: (613) 533-2813; FAX: (613) 533-6830;

Email: greerp@post.queensu.ca.

Abstract Count: 199

Abstract

Expression of a "gain-of-function" mutant human *fps/fes* transgene (*fps^{MF}*) encoding an N-terminally myristoylated Fps protein tyrosine kinase (MFps) gave rise to hyper-vascularity in mice. We present here a detailed characterization of the physiological and biochemical properties of this hyper-vascular phenotype. *fps^{MF}* mice exhibited 1.6-1.7 fold increases in vascularity that was attributable to increases in the number of secondary vessels. Morphologically, vessels were larger and exhibited varicosities and disorganized patterning. Functionally, vessels exhibited defects in histamine-induced permeability. *fps^{MF}* mice also displayed cardiomegaly, decreased arterial pressure and increased ventricular atrial natiuretic peptide expression. Biochemical characterization of endothelial cell lines derived from *fps^{MF}* mice revealed that MFps was activated in response to vascular-endothelial growth factor (VEGF) and platelet-derived growth factor (PDGF). However, activation of wild type Fps was not detected in response to these agonists, suggesting that MFps caused abnormal sensitization to VEGF and PDGF signaling in endothelial cells. We propose that MFps-induced sensitization contributes to aberrant angiogenic signaling and underlies the observed hyper-vascular phenotype of *fps^{MF}* mice. These phenotypes recapitulate important aspects of the vascular defects observed in both VEGF and Angiopoietin-1 transgenic mice. Therefore, the *fps^{MF}* line of mice constitutes an important new murine model for the study of angiogenesis.

2

Introduction

Vasculogenesis involves the development of a primary vascular plexus that is predominantly, but not exclusively, dependent on vascular-endothelial growth factor (VEGF) and basic fibroblast growth factor (bFGF) (reviewed in[1-4]). These growth factors play key roles in vasculogenesis by influencing angioblast differentiation following their induction from mesodermally-derived hemangioblasts[1]. The primary plexus then undergoes angiogenesis, a process of vascular expansion and remodeling that involves vessel sprouting, bridging and intussusception. The VEGFs and angiopoietins are critical for vascular development and are thought to play coordinated and complementary roles. VEGF induces endothelial sprouting, while angiopoietin-1 (Ang-1) and angiopoietin-2 (Ang-2) play antagonistic roles in vessel stabilization and destabilization, respectively. Final maturation of the vascular network, or arteriogenesis, requires mesenchymal derived induction and recruitment of pericytes followed by pericyte proliferation and migration in a longitudinal fashion to provide a smooth muscle coating to nascent endothelial tubes (reviewed in [1]). Mural cell coatings provide stabilization to newly emergent vessels by providing viscoelastic and vasomotor properties, protection against rupture and regression, and hemostatic control. Transforming growth factor-β (TGFβ) and platelet-derived growth factor (PDGF)-B are thought to play important roles in arteriogenesis. TGFβ has been implicated in mesenchymal to pericyte differentiation, pericyte recruitment, extracellular matrix (ECM) deposition, and inhibition of endothelial proliferation, while PDGF has been associated with smooth muscle proliferation and migration.

PDGF mediates a diversity of biological effects including wound healing[5], angiogenesis[6] and atherosclerosis[7]. Regulation of this diversity of post-natal and developmental processes occurs through PDGF-mediated effects on proliferation, survival and chemotaxis[8] (reviewed

in[9,10]). PDGF is also oncogenic, although its cellular transforming ability has been shown to be dependent on the particular genetic background of the cell[11]. Genetic analysis of PDGF and its cognate receptors has revealed critical requirements for this ligand/receptor pair in embryonic development. Genetic disruption of PDGF-B and PDGF receptor-β (PDGFRβ) resulted in lethality induced by sudden onsets of microvascular hemorrhaging; possibly a result of compromised vessel integrity related to a lack of pericyte/vascular smooth muscle cell (SMC) coating[12-16]. Other defects included impaired kidney and placental development and abnormal vascular morphogenesis and dilation of large and small caliper blood vessels[12,14-17]. In the brain, failed pericyte recruitment did not affect microvessel density length and branching, but was associated with endothelial cell hyperplasia, abnormal EC ultrastructure and increased transendothelial permeability[12].

Fps/Fes (here after called Fps) and its closely-related homologue Fer comprise a unique family of non-receptor cytoplasmic tyrosine kinases[18]. Structurally, these kinases are defined by an N-terminal Cdc42 interacting Fer-CIP4 (FCH) homology domain, central coiled-coil and SH2 domains and a C-terminal tyrosine kinase domain[18,19]. Unlike Fer, which is ubiquitously expressed, Fps expression is more restricted and has been described in myeloid, endothelial, epithelial, neuronal and platelet lineages[20-22].

Early studies on Fps employed leukemic cell lines and focused on its proposed role in cytokine signaling and hematopoiesis. Surprisingly, initial genetic analyses of mice targeted with null (*fps*^{-/-}) or kinase-inactivating (*fps*[KR/KR]) mutations revealed only minimal effects on hematopoiesis[23,24]. These analyses however, did point to potential roles for Fps in innate immunity and inflammation[23-25].

4

Gain-of-function *fps* mice that transgenically expressed either viral Fps, or myristoylated human Fps (MFps) (*fps^MF* mice) were characterized by vascular hyperplasia, strongly suggesting that Fps might also regulate vasculogenesis and/or angiogenenic remodeling processes[26,27]. Recent observations of Fps activation upon engagement of the GPVI collagen receptor in platelets[28], and a bleeding defect in *fps^MF* mice (Sangrar et al., manuscript submitted) suggest an additional new role for Fps in thrombosis. Potential roles for Fps in both thrombosis and angiogensis are particularly intriguing in light of the understanding that angiogenesis and hemostasis are highly inter-related processes[29].

The initial study citing vascular hyperplasia in *fps^MF* mice was based primarily on immunohistochemical analysis of brown adipose tissue[27]. Here we have used quantitative fluorescence intravital microscopy (FIVM) in the cremaster muscle and two-photon confocal fluorescence microscopy in the liver and brain to characterize the vascular phenotype in greater detail. We report that the vascularity is elevated 1.6-1.7 fold in *fps^MF* mice; which is predominantly a function of increased number and branching of medium-sized (2nd order) blood vessels. In addition, we observed unexpected and striking defects in the morphological characteristics of the vasculature including highly disorganized and tortuous vascular patterning. Moreover, permeability defects in response to the inflammatory mediator histamine were observed, supporting a role for Fps in the regulation of cell-cell adhesion. Lastly, we report that VEGF and PDGF activated MFps, but not Fps, in endothelial cells derived from *fps^MF* mice. This suggested that myristoylation of Fps conferred an oncogenic sensitization of endothelial cells to VEGF and PDGF.

Materials and Methods

Materials

Recombinant platelet-derived growth factor-B (PDGF) and VEGF were obtained from R&D Systems Inc. Recombinant bFGF was generously provided by the National Cancer Institute (Rockville MD). Anti-Myc ascites was prepared from MYC 1-9E10.2 (ATCC).

Mice

Transgenic mice (*fps^MF*) tissue-specifically over-expressing a myristoylated form of Fps (MFps) in an out-bred CD-1 background were housed at the Animal Care Facility at Queen's University, Kingston ON. The derivation of this line has been previously described[27]. All experimental procedures conformed to the guidelines of the Canadian Council of Animal Care and were approved by the Queen's University Animal Care Committee.

Fluorescence Intravital Video Microscopy (FIVM)

Male mice were anesthetized with sodium pentobarbital (65 mg/kg intraperitoneally) and the right external jugular vein was canulated for subsequent administration of fluorescein isothiocyanate (FITC) labeled-albumin (Sigma). An incision was made at the base of the scrotal sack allowing the right testicle and surrounding cremaster muscle to be exposed. All fascia were removed carefully, and a vertical incision was made in the cremaster muscle through the length of the testicle. The epididymis and testicle were freed from the muscle and allowed to retract into the abdominal cavity. The muscle was then held using 4-0 surgical silk over the viewing port of the platform and suffused with modified-Krebs buffer. After surgical preparation, the animal was placed on the stage of a triocular ELR-Intravital Microscope (Wild-Leitz). In each animal, a suitable area of cremasteric muscle vessels was isolated for study. The images were captured with a SONY DXC-390m 3ccd color video camera and a Matrox Meteor II Multi-

Channel (RGB) Image Capture card. On-line video image processing and analysis was performed with Image-Pro Plus 4.0 software (Media Cybernetics).

Microvascular quantification of cremaster vascular networks

The vascular network of the cremaster muscle was quantified by two methods. FITC-albumin was injected intravenously (25mg/kg), enabling fluorescence-based visualization of the vascular network using FIVM. Microscope images of cremaster muscle preparations were collected sequentially for the entire exteriorized muscle. After analysis, image composites were constructed to show the entire area studied (approximately 6.5 mm^2). Vascular networks were manually traced on the individual captured images and the total length of all vessels was then calculated per unit tissue area. Alternatively, bitmap intensity analysis using Image-Pro Plus imaging software was employed to obtain vascular area estimates from composite images of cremaster muscle. Vascular areas were computationally determined on the basis of selection of pixels that fell within threshold intensity ranges corresponding to vascular areas in which FITC-labeled albumin was present. Identical threshold intensity ranges were employed for all composite images. From this data, 3-D histograms were charted for each genotype and ratios of vascular to tissue area were calculated.

Brain and hepatic vascular network imaging

FITC-albumin (25 mg/kg) was administered by venous canulation into anesthetized mice. Approximately 3 minutes post-injection, identical regions of brain and liver tissue were surgically removed and immediately visualized using a Leica TCS SP2 multi-photon microscope. Images were captured at steps of 1.5 μm to a total tissue depth of 75 μm. Capture images were stacked and rendered using ImageJ 1.26 image processing software.

Microvascular permeability studies

Microvascular permeability of post-capillary venules from cremaster muscle preparations was assessed by the quantification of FITC-albumin extravasation in response to histamine suffusion. Immediately after FITC-albumin administration (25 mg/kg, i.v.), modified Krebs solution was suffused at a constant rate for 15 minutes followed by suffusion of 10^{-3} M histamine buffered in modified-Krebs solution for an additional 15 minutes. Images were captured automatically every 15 sec. post-FITC-albumin administration. Captured images were converted to 8-bit gray scale (0-255 pixel assignment) and mean optical intensity was measured in a 220x270 μm "area of interest" (AOI) encompassing the extravascular space adjacent to the post-capillary venule being studied. Increases in vascular permeability were quantified as a measurable shift in mean optical intensity in the AOI as a result of increasing FITC-albumin accumulation in the interstitial space adjacent to the post-capillary venule under examination.[30]

Heart rate and blood pressure determination.

Mice were anaesthetized with an intraperitoneal injection of sodium pentobarbital (60 mg/kg diluted 50% with saline) and mechanically ventilated (Harvard Apparatus) with 40% oxygen at a constant volume of 8-10 ml/kg and a frequency of 115 breaths/min. These ventilator settings result in a peak airway pressure of 6-8 cmH$_2$O, and have been shown previously to provide normal arterial blood gases[31]. A low volume catheter line (<10 μl) was placed in the abdominal vena cava for intravenous administration of anaesthetic and other drugs (injection volumes of 1 ml/kg). Electrocardiogram electrodes were placed subcutaneously for the measurement of heart rate (HR) and a blood pressure transducer (Mikro-Tip® Catheter 1.4F, Millar Instruments, TX) was inserted into the left branch of the carotid artery for measurement of arterial blood pressure. Mice were paralyzed with doxacurium chloride (0.25 mg/kg) (Wellcome Medical Division, ON)

to prevent respiratory efforts. Arterial blood pressure and electrocardiogram signals were acquired by a computer data acquisition package (CODAS DATAQ, Akron, OH) at a sampling frequency of 1000 samples•s^{-1}•channel^{-1}. Acquired data was analyzed using peak detection software and data were imported to a spreadsheet for calculation of HR and mean arterial blood pressure (MAP).

Methylcholine stimulation of heart rate and blood pressure

Increasing doses of methylcholine (MCh) (5, 25, 50, and 100 µg/kg) were injected intravenously into anaesthetized, paralyzed (doxacurium chloride 0.25 mg/kg), and ventilated mice 2 minutes post volume history maneuvers to total lung capacity. Average values for HR, diastolic and systolic blood pressures were calculated for 30 s of data acquired prior to injection of MCh (control) and in 10 s bins for 140 s after MCh injection. Peak responses to MCh were measured at 30 s post injection.

ANP Northern

Northern blots for ANP were performed as previously described[32] with the following modifications. The template for *in vitro* antisense riboprobe labeling was produced by PCR using the following primers: sense 5'-AACCCACCTCTGAGAGAC-3', antisense 5'-GGAAGCTGTTGCAGCCTA-3'. The PCR product was cloned into the pCRII vector (Invitrogen, Carlsbad, CA). The ANP/pCRII plasmid was linearized with XhoI and SP$_6$ RNA polymerase was used for riboprobe labeling.

VEGF and PDGF stimulation of C166 endothelial cell lines

C166 endothelial cells were isolated from day-12 yolk sacs of *fps^{MF}* mice[33]. C166 and derivative lines were grown in DMEM, 10% fetal bovine serum (Gibco). VEGF and PDGF stimulation experiments were performed on native C166 lines and on C166 cell lines ectopically expressing

C-terminal-Myc-epitope-tagged variants of Fps using a retroviral transduction protocol previously described[34]. The following pMSCV (murine stem cell virus) constructs encoding variants of Fps were utilized: 1) *pMSCV-fps-myc*, myc-epitope-tagged wild type Fps (C166-Fps-Myc cell line); and 2) *pMSCV-fps^{MF}-myc*, myc-epitope-tagged variant of Fps containing an N-terminal Src-like myristoylation target sequence[27] (C166-MFps-Myc cell line). Cells were starved overnight in serum-free DMEM, stimulated with increasing concentrations of PDGF (0-3.3 nM) or VEGF (0-2.4 nM) (R&D Systems Inc) for 2.5-5 min and lysed in PLCγ lysis buffer containing a cocktail of protease inhibitors[35]. Cell lysates were either immunoprecipitated (IP) with FpsQE anti-sera specific for Fps and Fer, with FerLA anti-sera specific for Fer[20], or with anti-Myc ascites (anti-Myc). In some cases, soluble cell lysates (SCLs) were analyzed directly by immunoblotting (IB). IPs and SCLs were subsequently probed with the following antibodies according to manufacturer instructions or as described previously[20]: FpsQE, FerLA, anti-Myc, and anti-phospho-tyrosine (Santa Cruz Biotechnology, Santa Cruz, CA).

Results

Reduced embryonic viability of fps^{MF} mice

Knock-outs of VEGF, Ang-1, PDGF-B and their respective receptors have displayed moderate to severe embryonic lethality due to defects associated with compromised vasculogenesis and/or angiogenesis. Initial attempts to generate *fps^{MF}* transgenic mice suggested that moderate levels of MFps expression were well tolerated, but higher levels could cause embryonic or perinatal lethality[27]. The life span of the established *fps^{MF}* transgenic mouse strain ranges from 1-14 months, with premature death occurring at a median age of 7 months due to systemic effects of hyperplasia, including internal hemorrhaging[27]. The dramatic variation in life span, coupled with well-documented examples of embryonic lethality associated with abnormal vascular development, led to the speculation that some *fps^{MF}* mice may be dying *in utero*. In order to test this, we performed genotypic analysis of offspring derived from hemizygous *fps^{MF}* (♂) x *wt* (♀) breeding pairs. This revealed a statistically significant increase in the expected number of *wt* vs hemizygous *fps^{MF}* progeny [57:43 *vs* expected 50:50 ratio (*wt:fps^{MF}*) ($\chi 2$ = 3 x 10^{-6}] suggesting that a number of *fps^{MF}* mice may be dying *in utero*, presumably due to complications associated with systemic hyperplasia.

Phenotypic similarities of fps^{MF} mice with VEGF and Ang-1 transgenic mice

Over-expression of either Ang-1 or VEGF from the keratin 14 promoter in mice (K14-Ang1 and K14-VEGF) gave rise to tortuous vessel morphology, aberrant patterning and increased vessel density in the skin.[36-38] Ang-1 transgenic mice also displayed excessive dilation of blood vessels[37,38]. Co-expression of Ang-1 and VEGF produced an additive effect in which both increased vessel density and excessive dilation was observed[38,39]. The phenotypes exhibited by these transgenic lines were characterized by redness of the skin on the ears and on the underside

11

of the nose and feet[36-38]. Although transgenic targeting was not skin specific in *fps^MF* mice, a remarkably similar redness of skin was also observed, pointing to the existence of similar defects in vascular morphology (Figure 1). Moreover, this redness was also observed in *fps^MF* neonates (Figure 1D) suggesting that defects in vascularity arise during embryogenesis. This is consistent with statistical evidence of *in utero* death and with isolation of immortalized endothelial (C166) cells from day 12-14 yolk-sacs of these mice[33].

Hypervascularity and aberrant vascular patterning in fps^MF mice

The initial hyper-vascular characterization of the *fps^MF* mouse line was based solely on immunohistochemical analysis of vessel density in the brown adipose tissue of neonatal animals and on the presence of hemangiomas[27]. Here we have greatly extended this analysis, showing abnormal vascular patterning, excessive tortuosity and vascular varicosities in the blood vessels of *fps^MF* mice (Figures 2). Morphometric analyses of the vascular network in cremaster muscle preparations visualized by intravascular perfusion of FITC-albumin showed a 1.6-fold ($p = 0.0005$) increase in total vascular area in *fps^MF* mice (Figure 3A), and a corresponding 1.7-fold ($p = 0.05$) increase in total vascular length per unit tissue area (Figure 3B). Visual inspection of these composites indicated that hyper-vascularity was primarily attributable to increased branching of vessels of secondary order (arterioles and venules) emanating from primary vessels (Figure 2). This is quantitatively depicted in the volumetric (red) and linear (yellow) intensity profiles of each composite image, which shows increased signals of intermediate FITC-albumin intensity in regions between primary vessels in *fps^MF* mice (Figure 2). Visual inspection of capillary density was partially limited by resolution; however, comparable or very modest decreases in capillary density were discernable (data not shown). Interestingly, abnormal vascular patterning was still evident at the level of capillaries (data not shown). Since intensity

12

values correlate with vessel size in these plots, a frequency distribution profile of vessel size can be generated in the absence of spatial information. This type of analysis revealed that vessels of increased size occurred with greater frequencies in fps^{MF} mice (Figure 3C). Interestingly, this morphometric analysis also predicted fewer of the smallest sized vessels in fps^{MF} mice, affirming our subjective observation of modest decreases in capillary density in fps^{MF} mice. Thus, fps^{MF} mice appear to exhibit vascular abnormalities that are reminiscent of the phenotypes in K14-VEGF and K14-Ang-1 mice in that they display defects in patterning, vessel density, branching and size.

Vascular hyperplasia and malformations in brain and liver of fps^{MF} mice

We next wanted to examine the extent of vascular hyperplasia and malformations in other tissues of fps^{MF} mice. We employed two-photon laser confocal microscopy for this purpose and focused on brain and hepatic tissue obtained from FITC-albumin injected mice. Images of brain tissue of equivalent thickness showed gross aberrations of the type observed in cremaster muscle in all orders of vessels including aberrant patterning, tortuosity and varicosities (Figure 4A, 4B). As observed in cremaster muscle, increased vascularity and branching appeared to be associated in particular with second order vessels in brain. This was more apparent when the images were rendered at different angles (Figure 4C, 4D). In some cases, primary vessels were larger, in agreement with the frequency distribution analysis in Figure 3C. In order to assess vessel density and morphology at the capillary level, we examined the sinusoidal hepatic capillaries under higher magnification (Figure 4E, 4F). Although we observed some degree of hyperplasia in the liver, it was not as striking as the hyper-vascularity in cremaster and brain. In addition, abnormal patterning and tortuosity was apparent to only a small degree in the liver. These data suggest that a minor degree of excess branching and hyper-vascularity also occurs at the level of

hepatic capillary networks with minimal defects in vascular morphology and patterning. These observations conform with those in the brain and cremaster muscle and suggest that increases in vessel density are restricted to second order vessels, and that alterations in capillary density, morphology, and patterning were modest at best. The data affirms earlier predictions of tissue-wide hypervasuclarity[27] and further, demonstrated that MFps over-expression resulted in comparable but not wholly similar vascular aberrations in different tissues.

Enhanced vessel permeability in response to histamine

K14-VEGF mice and knockouts of Ang-1 and Tie-2 gave rise to leaky-vessel phenotypes while K14-Ang-1 mice gave rise to leakage-resistant vessels, suggesting an association between hyperplasia and defects in vessel permeability[38,40-42]. These associations prompted us to examine whether the vascular hyperplasia in *fps^MF* mice was also accompanied with permeability defects. We employed the permeability-inducing agent histamine, which induces cell contractility and has been shown to induce phosphorylation of endothelial adherens junctions proteins[43]. Histamine was directly suffused over cremaster preparations at a constant rate and plasma extravasation as a function of FITC-albumin intensity was measured. Upon suffusion, leakage began by approximately 150 sec and progressed linearly until saturation levels were reached due to upstream vasoconstriction or localized coagulation (*wt*, $n = 4$; *fps^MF*, $n = 5$; Figure 5D and 5E). We estimated the maximal extent of leakage, rate, and half-maximal time (P_{50}) of plasma extravasation for each mouse; these parameters are graphically depicted in the inset of Figure 5D. Using linear regression analyses, a mean 48% decrease in the rate parameter ($p = 0.003$) was calculated, consistent with the existence of a retarded rate of leakage in the blood vessels of *fps^MF* mice (Figures 5B, 5C). Non-linear regression analyses using a Hill 3-parameter sigmoidal function provided estimates of P_{50} and maximal levels of leakage. Interestingly, mean levels of

these parameters were both elevated 1.5-fold in fps^{MF} mice ($p = 0.005$ and $p = 0.048$ respectively; Figure 5A). The latter results suggested that although permeability rate was decreased, restoration of the vessel to resting permeability states could be delayed, resulting in overall increases in the levels of extravasated plasma. These data suggest that fps^{MF} mice may possess defects in cellular mechanisms that control cell-cell adhesion.

Cardiac abnormalities in fps^{MF} mice

Transgenic mice expressing a viral oncogenic *fps* allele gave rise to enlarged subcutaneous blood vessels and to cardiac abnormalities including cardiomegaly[26]. Cardiac abnormalities have also been observed in PDGF-B[15], Ang-1[42] and Tie2[41] knockouts. Examination of lateral and longitudinal cross-sections of the hearts of fps^{MF} mice revealed no overt differences in morphology suggesting normal heart function (data not shown). Heart rate was also normal in fps^{MF} mice (data not shown) however their mean heart size was increased by 10% ($p = 0.02$) (Figure 6A), probably as a result of the increased circulatory load requirements of hypervascularity. In addition, systemic mean arterial pressure (MAP) was reduced in fps^{MF} mice (*wt*, 55.4 ± 1.2 mm Hg, $n = 4$; fps^{MF}, 39.2 ± 1.6 mm Hg, $n = 4$; $p = 1.4 \times 10^{-7}$); this may be attributable to reduced peripheral vascular resistance as a result of increases in the degree of parallel blood flow.

Increased ventricular ANP mRNA levels

Cardiac hypertrophy and hypotension have been associated with increased atrial-natriuretic peptide (ANP) expression (reviewed in [44]). This peptide is secreted in the atrium and ventricle and elicits profound natiuresis and diuresis. Examination of ventricular *ANP* mRNA levels showed that message levels were elevated approx. 3.2-fold in fps^{MF} mice (Figure 6B).

Effect of the cholinergic agonist methylcholine on heart rate and blood pressure

We further explored the basis of cardiomegaly and system-wide reductions in blood pressure by examining heart function and vascular pressure in response to the muscurinic agonist methylcholine. Methylcholine induces NO secretion to cause vasodilation peripherally and engages the M2 muscurinic receptor expressed on myocytes in the atria and ventricle to induce bradychardia (reviewed in [45-47]). Increased sensitivity to methylcholine-induced bradychardia was observed in *fps^MF* mice (Figure 7A). Methylcholine also induced dose-dependent decreases in mean arterial pressure (MAP) in both *wt* and *fps^MF* mice (Figure 7B). The *fps^MF* MAP response profile to methylcholine was similar to that observed in *wt* mice suggesting that dilation capacity of blood vessels is intact in *fps^MF* mice. When the vasoconstrictor phenylephrine was administered, increases in MAP were also comparable indicating that vessel constriction capacity, as well, is normal in *fps^MF* mice (data not shown).

Fps is activated downstream of PDGF in C166 endothelial cells

Preliminary attempts to delineate the molecular basis of defective angiogenesis involved the testing of key angiogenic factors on C166 endothelial cells derived from *fps^MF* mice. Stimulation of C166 cells with bFGF or with Ang-1 conditioned media did not elicit Fps or MFps activation in this cell line (data not shown). When C166 cells were stimulated with PDGF-B we observed a striking response in the global tyrosine phosyphorylation profile (Figure 8A). An identically potent response was observed in a hemangioendothelioma cell line (EOMA) (Figure 8B) suggesting that the PDGFR is expressed in both lines of endothelial cells. Subsequent immunoprecipitation and Western blot analyses revealed a dose-dependent increase in tyrosine phosphorylated Fps/MFps species in response to PDGF in C166 cells (Figure 8C). In EOMA cells, basal levels of activation of Fps (and Fer) were elevated and remain unchanged with

increases in PDGF-B doses (data not shown). Quantification of the Fps phosphotyrosine signal revealed a sigmoidal activation profile indicative of an ultra-sensitive response to PDGF[48,49] (Figure 8F). This was suggested by a Hill coefficient parameter (n_H) of 2.43, obtained by non-linear regression using a Hill 3-parameter function. This parameter has been utilized to differentiate between the sensitivity of responses in biological systems where n_H values of one, represent Michaelis-Menton-like (hyperbolic) sensitivity whereas n_H values below and above one represent sub- and ultra-sensitivity thresholds, respectively.[48,49]

Fer (94 kDa) migrates closely with Fps and MFps (both approximately 92 kDA) and these kinases are routinely visualized as a doublets on SDS-PAGE[20,21]. The ratio of Fps plus MFps to Fer expression in C166 cells is extremely large, resulting in the immunoprecipitation (IP) of mainly MFps and Fps using an anti-Fps antibody (FpsQE) that has cross-reactivity with Fer. This is demonstrated in Figure 8D where a band corresponding to Fer in an IP using a Fer-specific antibody (FerLA) is absent in the adjacent FpsQE immunoprecipitates. Nonetheless, since Fer has been shown to be activated by PDGF[50], we took precautionary measures and examined the degree to which Fer activation might contribute to phosphotyrosine signal generated in the Fps/Fer IPs shown in Figure 8C. Inducible activation of Fer was barely observable at concentrations of PDGF as high as 1.6 nM and 2.4 nM (Figure 8D and 8E) suggesting that the PDGF-induced phosphotyrosine signal in Fps/Fer IPs is predominantly due to Fps and/or MFps activation.

MFps sensitizes C166 endothelial cells to PDGF signaling

In order to delineate the relative proportions of activation of endogenous MFps and Fps by PDGF we utilized C166 cell lines that had been transduced with retroviruses encoding myc-epitope-tagged Fps (Fps-Myc) and MFps (MFps-Myc). These epitope tagged variants migrate at

approximately 120 kDa and could be easily distinguished from endogenous Fps and MFps signals. As expected, dose-dependent increases in tyrosine phosphorylation were seen in the band corresponding to endogenous Fps and MFps in both C166 lines expressing myc-epitope-tagged variants of Fps (Figures 9A, 9B; lower band). Unexpectedly, we did not observe tyrosine phosphorylation of Fps-Myc in the cell line expressing this variant (Figure 9A). However, we observed dose-dependent tyrosine phosphorylation of MFps-Myc (Figure 9B). This demonstrated that only the myristoylated (activated) MFps variant undergoes activation in response to PDGF. The latter results were consistently observed regardless of whether anti-Myc (not shown) or FpsQE was used for immunoprecipitation. These data suggest that MFps mediates an ultra-sensitive response to PDGF signaling in endothelial cells from fps^{MF} mice.

VEGF transiently activates MFps but not Fps in C166 cells

Treatment of C166-Fps-Myc cells with 0-2.4 nM VEGF induced a modest activation of MFps. This activation was specific to MFps since Fps-Myc activation was not observed (Figure 10A). Thus, as was the case with PDGF, MFps also sensitizes C166 cells to VEGF signaling. Unlike the ultra-sensitive response to PDGF however, the activation of MFps by VEGF was weak and transient at both 2.5 and 5 min (Figure 10B).

Discussion

Cardiovascular defects are frequently associated with defective vascular development, both at the cellular and organ level[15,42,51-53]. With the exception of minor cardiomegaly, this did not appear to be case with *fps^{MF}* mice, which appeared to have relatively normal heart development and function. Since vasculogenesis and early heart development are spatially and temporally linked, and since cardiac structure is relatively intact in *fps^{MF}* mice, we speculate that the vascular defects in *fps^{MF}* mice may predominantly manifest during the angiogenic remodeling phase of vascular development. This is consistent with the observation of branching and patterning defects in vessels of secondary but not primary order, and with an apparent lack of vascular defects in the yolk sacs of *fps^{MF}* mice (data not shown).

The observed cardiomegaly in *fps^{MF}* mice may be due to chronic effects of load arising from increased blood volume levels that can be expected with hypervascularity. Expansion of blood volume also leads to natriuresis, which attempts to restore normal levels of blood volume. Indeed, a natriuretic response was suggested by the significant increase in ANP *mRNA* levels. ANP also has been shown to mediate potent antihypertensive actions which might explain the observed constitutive reductions in MAP (reviewed in [54]), although reduced MAP may also be attributable to increased parallel blood flow.

Both VEGF and Ang-1, when over-expressed in the skin, gave rise to increased vascularity; however, each was associated with unique physiological and morphological aberrations of the vasculature[37,38]. Increased vascularity was predominant in K14-VEGF mice, while vessel enlargement was predominant in K14-Ang-1 mice[38]. In addition, K14-VEGF mice had leaky vessels in response to challenge, while K14-Ang-1 mice had leakage-resistant vessels[38]. As expected, K14-VEGF/Ang-1 double transgenic mice produced complementary

effects resulting in significant increases in both vessel number and size, accompanied with reduced leakiness[38,39]. In this regard, *fps^MF* mice exhibited significant parallels with both K14-VEGF and K14-Ang-1 transgenic mice. Specifically, *fps^MF* mice displayed pronounced hyper-vascularity, evidence for vessel "leakiness" induced by challenge, and a general enlargement of vessels. These hyper-vascular and "leakage" phenotypes closely correlated with K14-VEGF mice, and they were consistent with both MFps activation downstream of VEGF, and with a potential positive effect on neoangiogenesis (Figure 11) and vascular permeability. The vessel enlargement phenotype correlated with the phenotype of K14-Ang-1 mice, although its degree of severity was comparatively modest in *fps^MF* mice. We were unable to observe direct Fps activation downstream of Ang-1 (data not shown), thus it is unlikely that vessel enlargement is due to direct effects of (M)Fps on Ang-1 signaling. However, it cannot be excluded that (M)Fps may indirectly modulate, perhaps through network cross-talk, components of the Ang-1 pathway that regulate vessel size.

PDGF is expressed on nascent endothelial cells during angiogenesis and acts in a paracrine fashion to potentiate SMC recruitment, migration and proliferation along nascent endothelial tubes[12-14,55,56]. As demonstrated in PDGF-B and PDGFR-β knock-outs, failure to recruit smooth muscle cells led to impaired arteriogenesis and hence compromises in vessel integrity resulting in an edematous phenotype[12,15,16,57]. Our data suggesting increased plasma-extravasation in *fps^MF* mice (Figure 5) is consistent with the possibility that MFps-mediated PDGF-signaling may have produced defects in arteriogenesis associated with abnormal SMC/pericyte recruitment and coating of vessels[12,58]. Such a possibility is also consistent with routine observations of edema in some aged *fps^MF* mice (data not shown). However, normal response profiles of methylcholine-induced reduction in arterial blood pressure in *fps^MF* mice

indicated normal vascular dilation and relaxation and argue for normal vessel smooth muscle morphology and function. Nonetheless, we cannot completely exclude the possibility of abnormal SMC recruitment/coating since arterial pressure responses are not necessarily a direct measure of vascular smooth muscle morphology and function.

Abnormal regulation of endothelial adherens junctions (AJ) might also underlie the observed permeability phenotype in *fps^MF* mice. Interestingly, histamine has been shown to augment vascular permeability by tyrosine phosphorylation of endothelial adherens junctions (AJ) components, resulting in dissociation of VE-cadherin from the actin cytoskeleton[43]. Precedence for a possible involvement of (M)Fps in AJ function stems from evidence implicating its closely related homologue Fer in regulating the tyrosine phosphorylation status of AJ components in neuronal[59], intestinal epithelial[60] and embryonic fibroblasts[61]. Thus, the observed reduction in rate of leakage and elevated levels of plasma-extravasation in response to histamine, could reflect an MFps-mediated slowing of the kinetics of AJ disassembly and reassembly. In other studies, targeted truncation of the cytoplasmic region of VE-cadherin, which interacts with β-catenin, did not affect vasculogenesis but impaired the subsequent angiogenic remodeling phase of murine vascular development[62]. In these mice, VEGFR-2-mediated survival signaling to Akt and Bcl2 was reduced due to reduced complex formation with VE-cadherin, β-catenin and phosphoinositide 3 (PI3)-kinase[62]. The implication of MFps in endothelial cell survival[33], coupled with the observed activation of MFps in VEGF signaling suggested therefore that MFps may influence endothelial cell survival through signaling mechanisms involving VEGFR-2/VE-cadherin/β-catenin complexes.

Fps and Fer are the only members of the protein-tyrosine kinase family that possess the FCH domain. This domain was first identified in the Cdc42-interacting protein (CIP4), a

downstream target of the Rho GTPase Cdc42 that has been implicated in signaling and cytoskeletal control[18,19]. Intriguingly, several studies have implicated Rho GTPases including Rac1, RhoA, and Cdc42 in regulating cadherin-mediated cell-cell adhesion. Cadherin regulation is thought to occur by action of Rac1 and Cdc42 on the cadherin-catenin complex, and by action of Rho on the actin cytoskeleton or other components. Hence the presence of an FCH domain in (M)Fps potentially implicates it in modulation of cadherin activity through a mechanism involving Rho-GTPases.

The similarity of phenotypes between K14-Ang-1 and K14-VEGF transgenic mice and *fps*^{MF} mice point to participation of Fps in an angiogenic mechanism involving both Ang-1 and VEGF. Current models of angiogenic remodeling propose that Ang-2 mediates vessel destabilization which primes subsequent neoangiogenesis in the presence of VEGF (Figure 11)[1,2,63]. Interestingly, studies elsewhere have shown that Ang-2 activates Fps, and that through Fps, Ang-2 stimulates migration and tube-like structure formation of endothelial cells[64]. Based on this observation, MFps might potentiate neoangiogenesis by promoting Ang-2 destabilization of blood vessels [STEP 1; Figure 11]. In the presence of Ang-2, VEGF promotes endothelial sprouting and branching[2]. MFps-mediated sensitization to VEGF signaling pathways might result in modulation of VEGF signaling effects leading to increased kinetics and magnitude of vessel sprouting and branching [STEP 2; Figure 11]. This process might be exacerbated by the presence of transformed-like properties of endothelial cells, as suggested by the ease of isolation of immortalized endothelial cell clones from *fps*^{MF} yolk sacs[33] (STEP 3; Figure 11).

Mouse models of Ang-1/Tie-2 and PDGF-B/PDGFRβ display defects in arteriogenesis associated with impaired pericyte recruitment[4,12-14,42]. It is thought that Ang-1, secreted by surrounding mesenchymal cells[65], acts on endothelial cells and induces PDGF secretion (Figure

11)[4]. PDGF has been proposed to bind to PDGFRβ on undifferentiated perivascular mesenchymal cells and/or on pericytes/SMCs to induce pericyte generation and subsequent migration and proliferation of pericytes along nascent endothelial tubes (Figure 11)[13]. In this context, an initial phase of endothelial PDGF autocrine signaling, followed by a switch to paracrine signaling has also been previously proposed[6,66]. However, whether or not PDGFRβ is normally expressed on endothelial cells has been controversial, especially since PDGF-B and PDGFβR knockouts do not appear to prevent formation of the endothelium[8,15,16]. Regardless, our data are consistent with the existence of an initial phase of PDGF autocrine signaling and further suggest that an ultra-sensitive activation response mediated by MFps would ensue during this phase. This activation may abnormally affect this phase of PDGF-signaling since endogenous Fps is not normally activated in response to this growth factor. Hence, potentiation of PDGF-autocrine signaling by MFps could elevate endothelial proliferative and survival indices, resulting in increased kinetics of branching and sprouting (STEP 4; Figure 11). Alternatively, it is possible that constitutive PDGFRβ or PDGF over-expression may be a property of the transformed endothelium in *fps^MF* mice. In this regard both PDGF and PDGFRβ over-expression have been shown to induce cell transformation[10,67-69]. Moreover, PDGFRβ has been shown to be highly expressed in the vasculature of gliomas but not normal brain, and it has been implicated in neovascularization of these tumors through autocrine mechanisms[67,68,70,71]. Thus, elevated PDGF-autocrine signals may also promote endothelial hyperplasia, an effect that would be exacerbated by MFps-mediated ultra-sensitivity to this growth factor (STEP 5; Figure 11).

Heterozygous VEGF deficient embryos (VEGF^{+/-}) generated by aggregation of VEGF^{+/-} embryonic stem cells with tetraploid supporting embryos exhibited intermediate severity of

23

blood vessel formation compared to VEGF$^{-/-}$ embryos, suggesting that VEGF dose-dependently regulated vessel development[72].   Another study showed that 3' UTR deletion of the VEGF gene gave rise to increased stability of VEGF transcript and to modest increases in VEGF expression resulting in embryonic lethality due to abnormal heart development[52]. These studies imply that tight dosage regulation of VEGF is critical for vascular development. Thus, it is conceivable that abnormal sensitization of MFps to VEGF signaling, even though weak and transient, might result in sufficient modulation of VEGF signaling to cause the severe defects in vascular development observed in *fps^{MF}* mice.

The physiological and molecular mechanisms underlying vasculogenesis and angiogenesis have been a subject of active interest given their therapeutic promise in heart disease and cancer.   Although recent genetic approaches have aided in the functional identification of numerous vasculogenic and angiogenic factors and in the development of working models of these processes, an understanding befitting practical therapeutic advancement is still elusive.   This is underscored by recent disappointments in clinical trials of several promising angiogenic inhibitors[73,74]. It has been difficult to generate appropriate animal models for the study of angiogenesis. Knockouts of VEGF, PDGF, Ang-1, Ang-2 and their respective receptors are embryonic lethal, and VEGF and Ang-1 transgenic mice have transgene-directed tissue-specific vascular phenotypes. *fps^{MF}* mice however are relatively viable and provide a suitable model for the study of both primitive and definitive vasculogenesis and angiogenesis in all tissues.   In addition, the process of arteriogenesis is an important aspect of angiogenic development and function; and in this respect, *fps^{MF}* mice might also constitute an important model for the study of this process.   Therefore the *fps^{MF}* mouse model will be important for further delineating the biochemical and physiological pathways that regulate both angiogenesis

and arteriogenesis, not only with respect to the role of Fps, but also with respect to key angiogenic and arteriogenic factors such as VEGF, Ang-1, Ang-2 and PDGF.
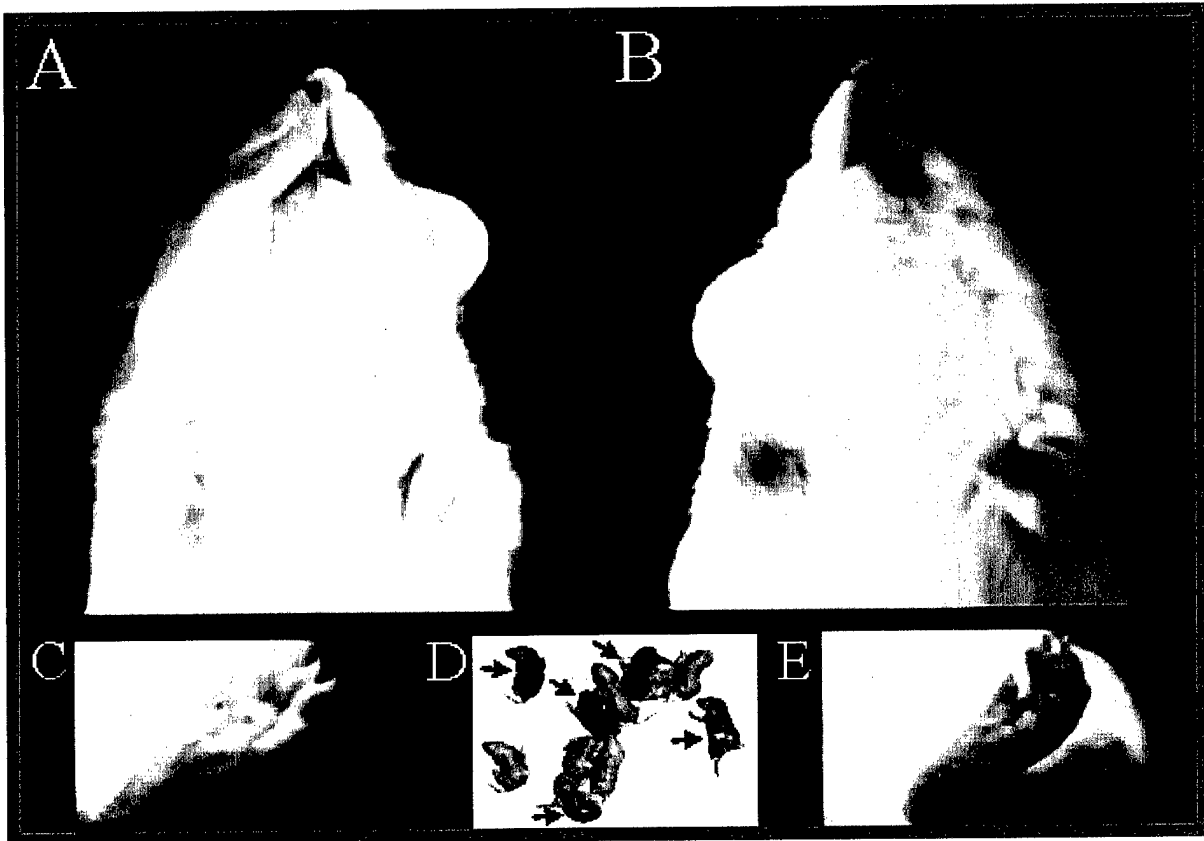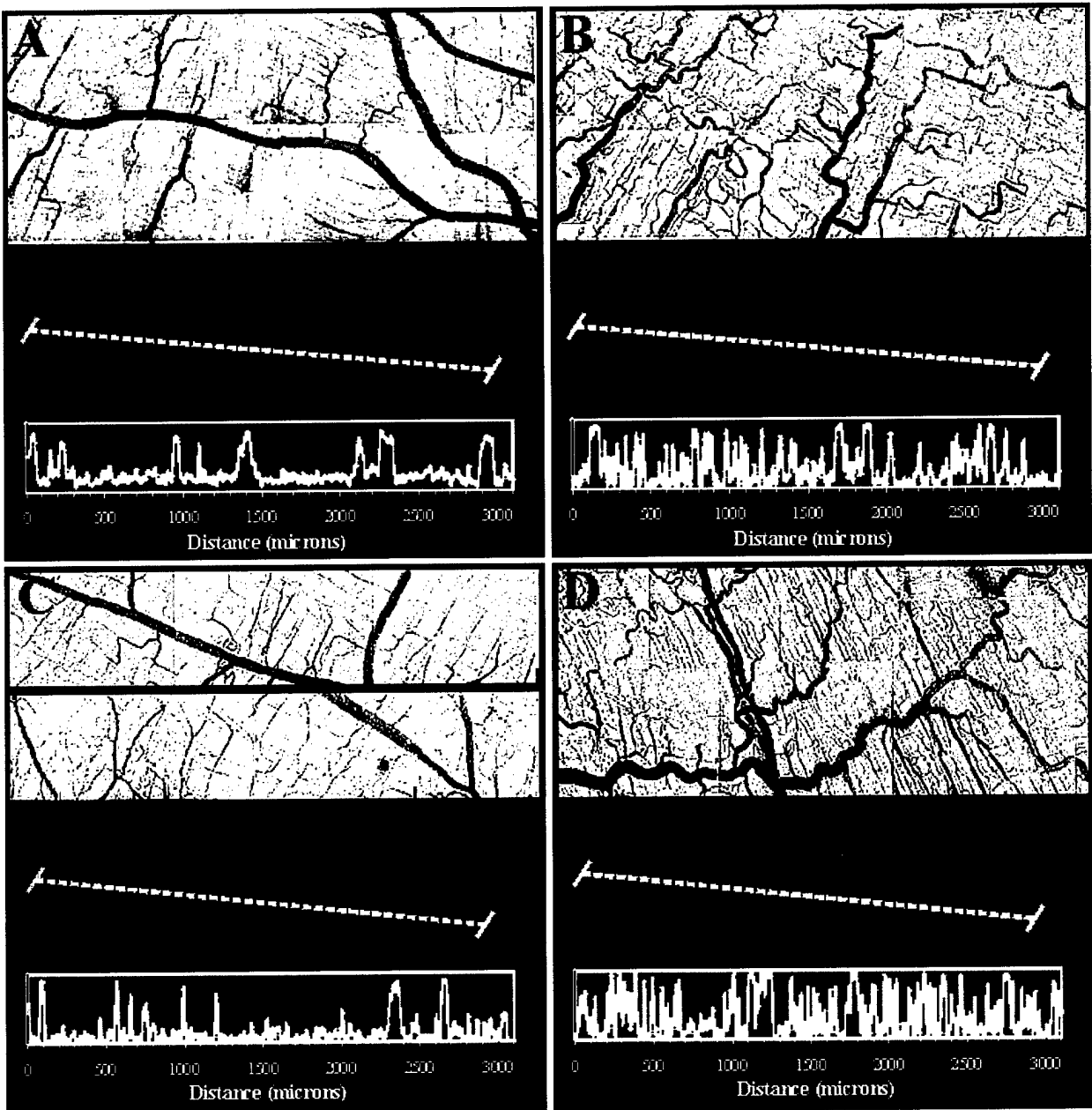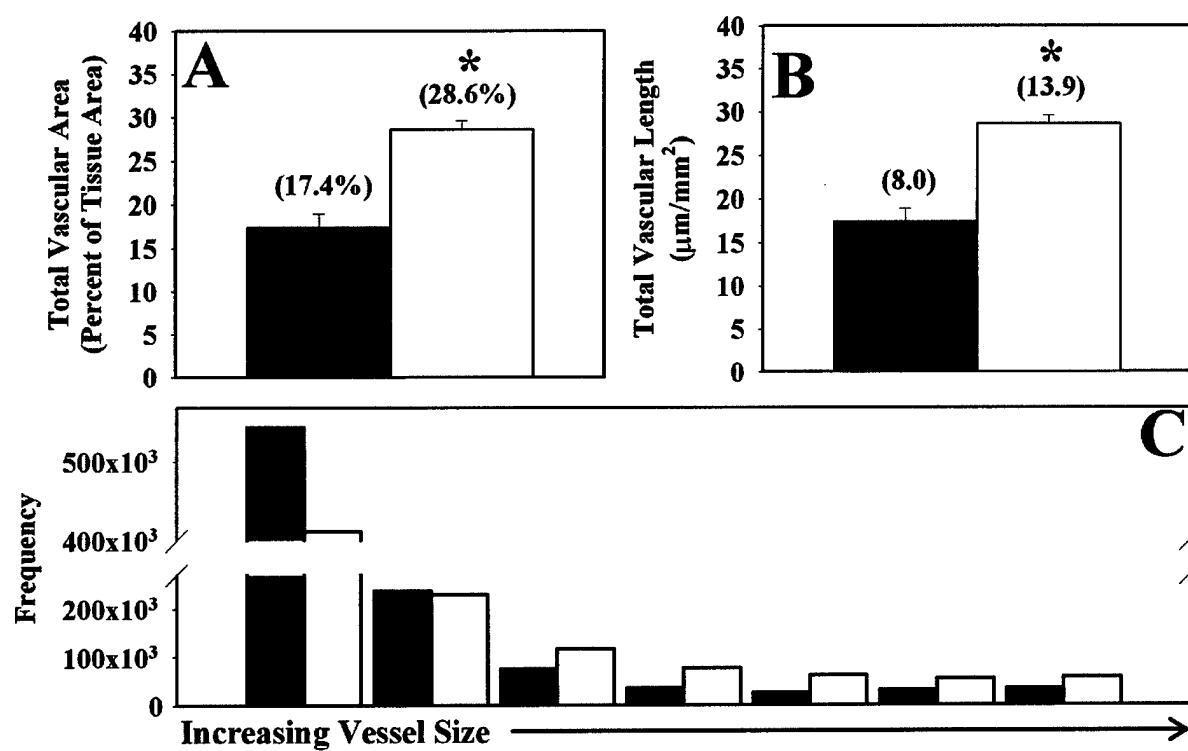
Figure 1

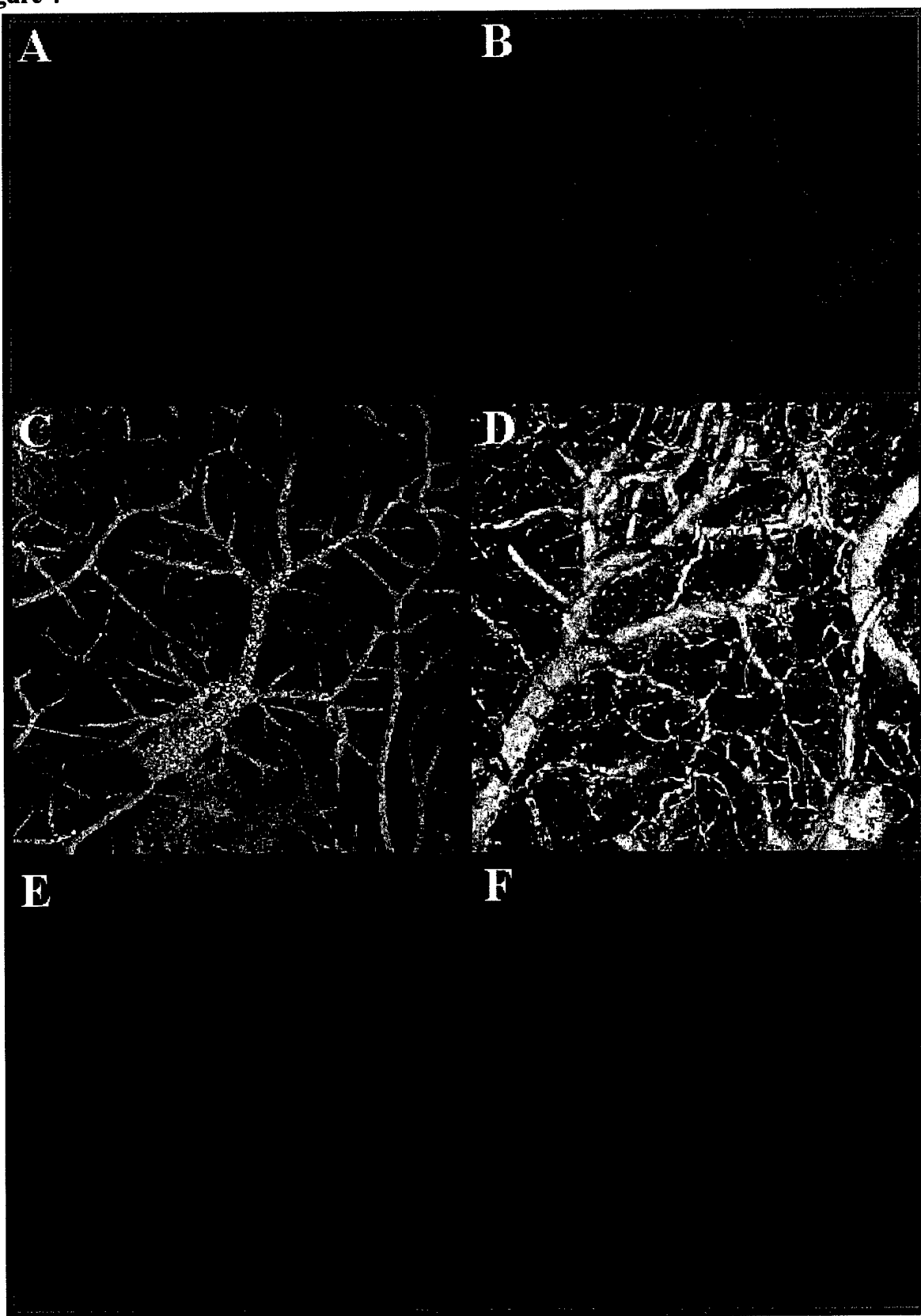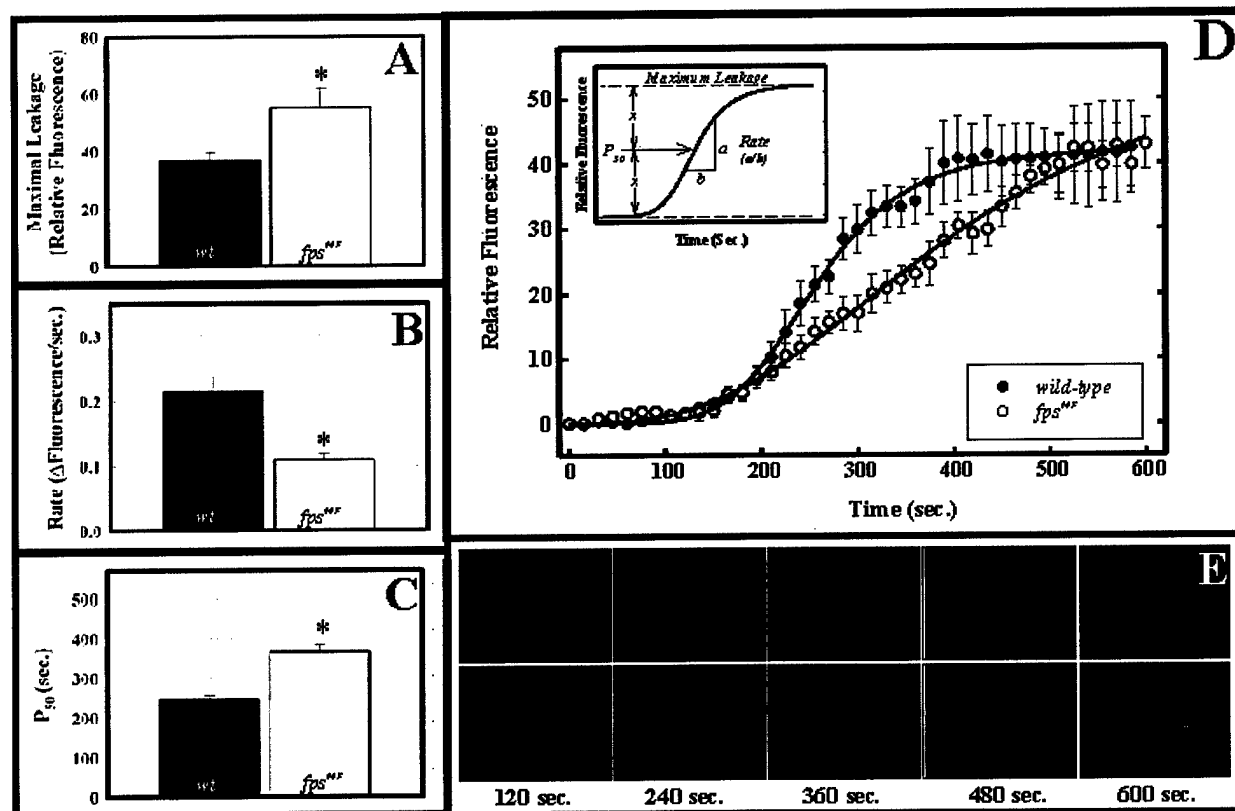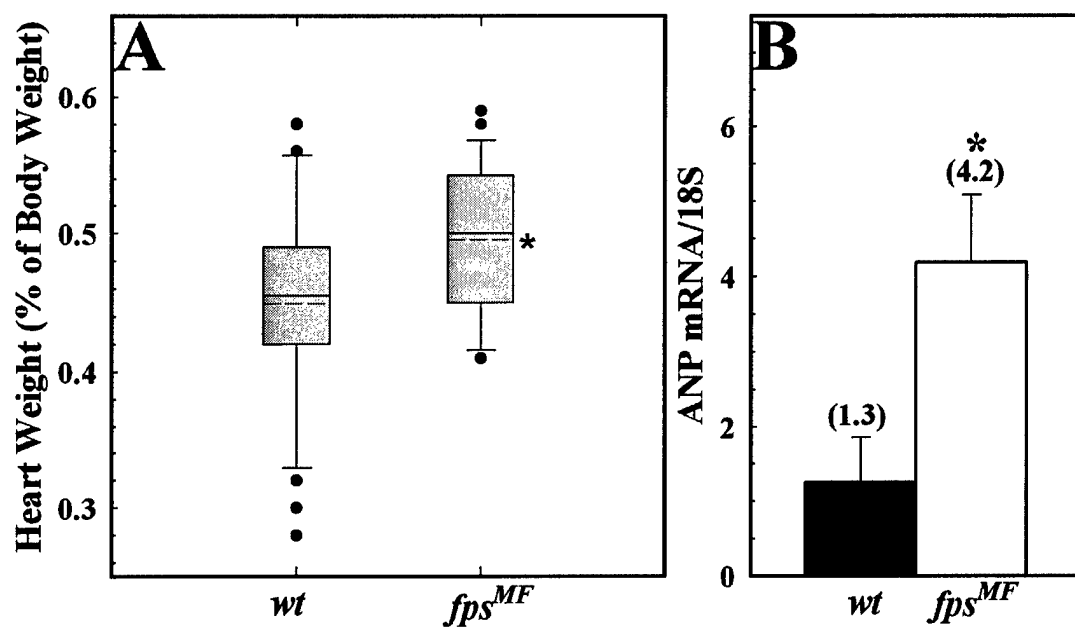**Figure 2**

Figure 3

Figure 4

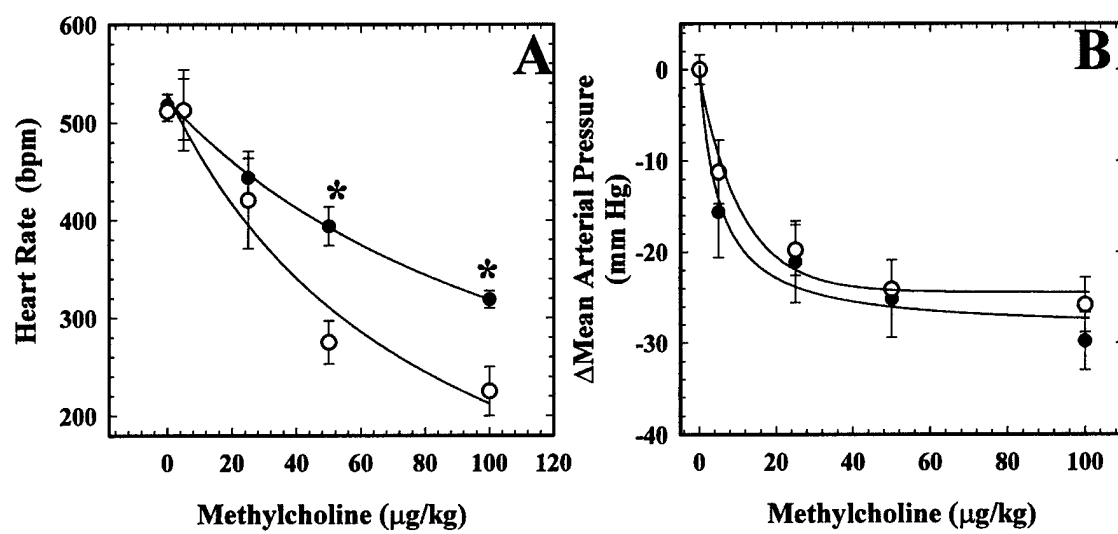**Figure 5**

Figure 6

Figure 7

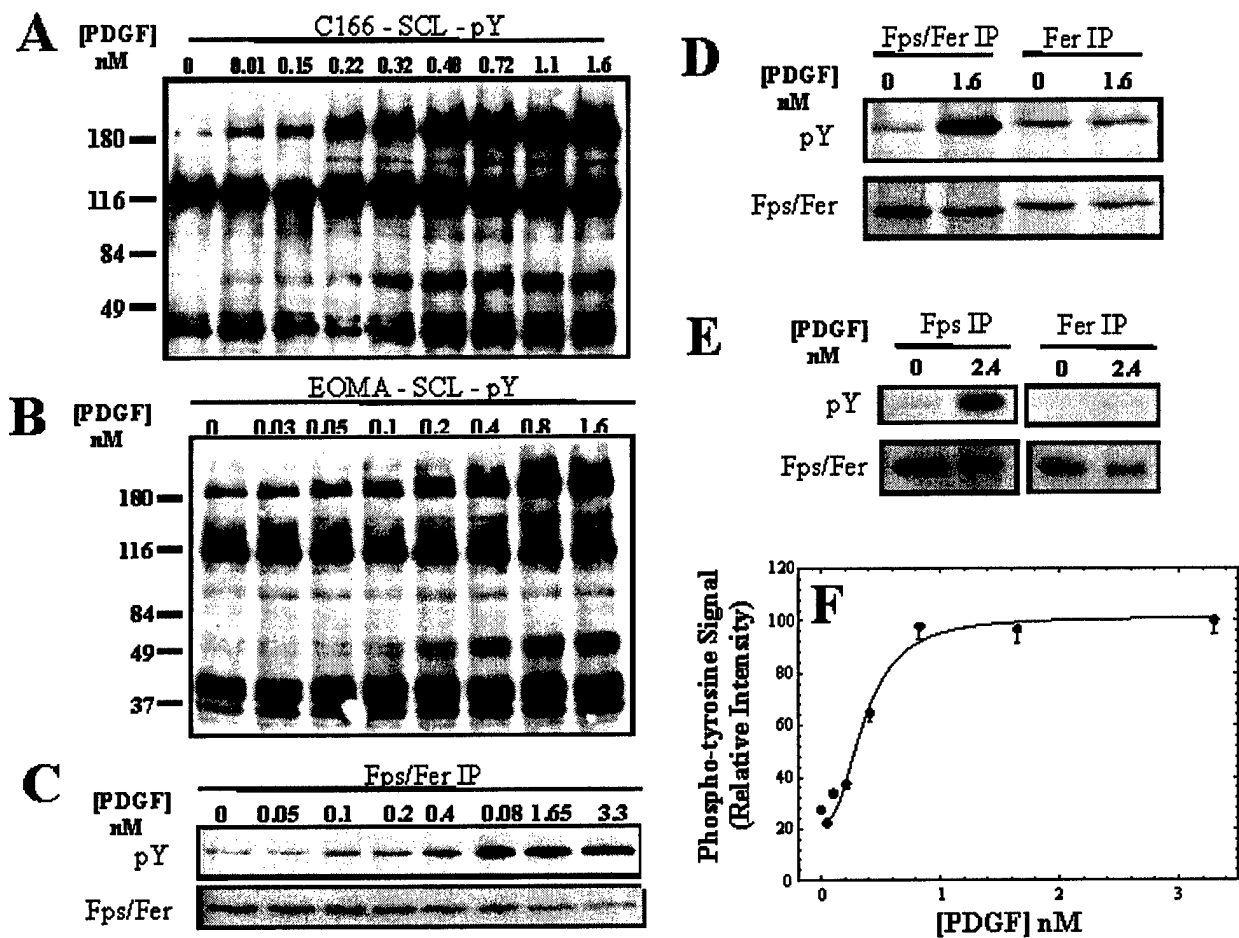**Figure 8**

Figure 9

Figure 10

A

Fps/Fer IP: C166-Fps-Myc, 5 min

| [VEGF] nM | 0 | 0.1 | 0.2 | 0.3 | 0.6 | 1.2 | 2.4 |

pY

Fps/Fer

B

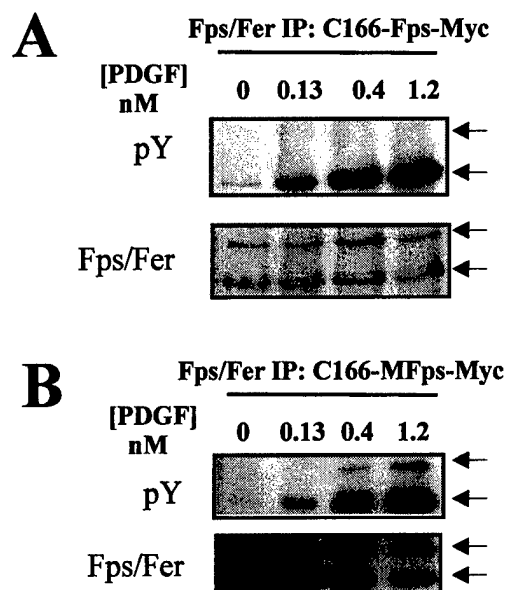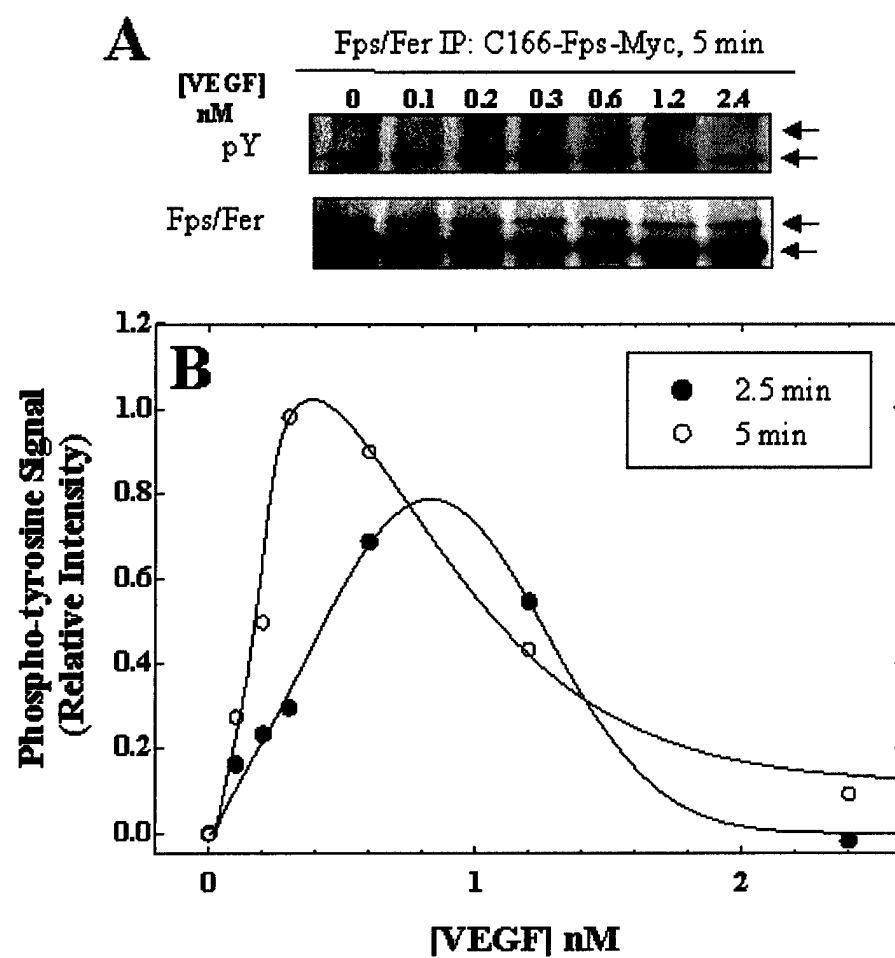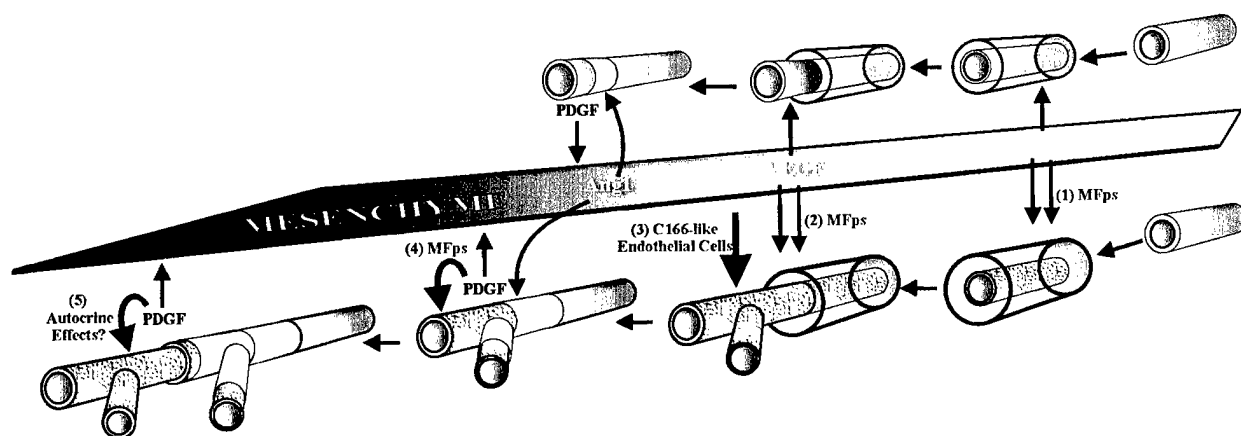Phospho-tyrosine Signal (Relative Intensity) vs [VEGF] nM

- ● 2.5 min
- ○ 5 min

Figure 11

Figure Legends

Figure 1. *Increased redness in skin of fps^{MF} mice resembles VEGF and Ang-1 over-expressing phenotype.* Increased redness of varying extent was observed in areas of skin lacking hair growth, which included regions of the nose and mouth, feet and tails (data not shown). Panels A and C, *wt*. Panels B and E, *fps^{MF}*. This redness was readily apparent in *fps^{MF}* neonates (Panel D, arrows).

Figure 2. *Comparison of vascular patterning and morphology in cremaster muscle using fluorescence intravital microscopy.* The upper section of each panel represents 2-dimensional composite images of vessel networks visualized by fluorescence microscopy (100X magnification). The middle section of each panel is the corresponding 3-dimensional fluorescence intensity plot of vessel networks in cremaster muscle. The bottom section of each panel represents a linear intensity plot of the region traversed by the yellow line shown in the middle section of each panel. These images clearly show that *fps^{MF}* mice exhibit pronounced hypervascularity, aberrant patterning and excessive tortuosity and vascular varicosities compared to their *wt* siblings. (Panels A and C, *wt*. Panels B and D, *fps^{MF}*). Also apparent were increases in the vascular density of vessels emanating from primary branches.

Figure 3. *Vessel density and size in cremaster muscle.* Morphometric analysis of composite images of cremaster muscle digitally captured at 100X magnification was utilized to yield estimates of vascularity. *fps^{MF}* mice were found to have a 1.6-fold increase in total vascular area [Panel A : *wt*, (black bars) 17.4 ± 0.9 %; *fps^{MF}*, (white bars) 28.6 ± 0.6 %; $n = 3$, $p = 0.0002(*)$] and a 1.7-fold increase in total vascular length per unit tissue area [Panel B: *wt*, (black bars) 8.0 ± 1.5 $\mu m/mm^2$; *fps^{MF}*, (white bars) 13.9 ± 0.8 $\mu m/mm^2$; $n = 3$, $p = 0.02(*)$]. Frequency

distribution analyses of intensity data captured by FIVM. Larger vessels occur with increasing frequency in fps^{MF} mice [Panel C: wt (black bars); fps^{MF} (white bars)].

Figure 4. *Comparison of vascular networks in brain and liver using two-photon confocal microscopy.* Images were obtained using two-photon confocal microscopy of whole tissue. Hypervascularity and tortuous vascular patterning was also found in the brain (Panels B and D: fps^{MF}; Panels A and C: wt; 100X; 75 µm) and liver (Panel F: fps^{MF}; Panel E: wt; 200X; 52 µm) of fps^{MF} mice. Also evident in these images were increases in the number of 2nd order vessels in the brain of fps^{MF} mice. (Compare Panel D to Panel C). Density of hepatic capillaries in fps^{MF} mice are modestly increased compared to wt mice (Compare Panel F to Panel E).

Figure 5. *Reduced vascular permeability in response to histamine in fps^{MF} mice.* Intravital microscopy was employed to monitor histamine-induced extravasation of FITC-albumin. Extravasation was measured as a function of total fluorescence intensity within a defined rectangular area encompassing both the vessel lumen and adjacent extra-vascular regions. Rate of FITC-albumin extravasation was readily visualized over time and showed that histamine-induced vascular permeability is compromised (Panel E: upper row, wt; lower row, fps^{MF}). This is quantitatively represented by temporal fluorescence profiles post-histamine suffusion [Panel D (Average ± SEM): fps^{MF} (o), $n = 5$; wt (●), $n = 4$]. Three parameters of the average fluorescence intensity profiles were assessed (Panel D: inset). The maximal leakage parameter was increased in fps^{MF} mice [Panel A: fps^{MF} (□), 55.2 ± 6.7; wt (■), 36.7 ± 2.7; $p = 0.048(*)$]. The rate parameter however was decreased [Panel B: fps^{MF} (□), 0.11 ± 0.01 ΔIntensity/sec; wt (■), 0.21 ± 0.03 ΔIntensity/sec; $p = 0.003(*)$]. Changes in the latter two parameters were reflected by increases in the half-maximal time of leakage (P_{50}) in fps^{MF} mice [Panel C: fps^{MF} (□), 364 ± 20 sec; wt (■), 245 ± 9 sec; $p = 0.005(*)$].

Figure 6. *Physiological characterization of cardiac function in fps^{MF} mice.* Heart weights were calculated as percentages of total body weight. Cardiomegaly was observed in fps^{MF} mice. [Panel A: Box plot representation of data: median (solid lines), average (dashed lines), 5th – 95th percentiles (symbols), 10th - 90th percentile (whiskers) 10th - 25th percentile (boxes); normalized heart weights (Average ± S.E.M); wt (4.9 ± 0.8 mo.), 0.45 ± 0.01, n = 28; fps^{MF} (4.8 ± 0.9 mo), 0.50 ± 0.01, n = 21; p = 0.02(*)]. Northern analysis revealed that ventricular ANP *mRNA* levels were increased 3.2-fold in fps^{MF} mice [Panel B: n = 3; p = 0.032(*)].

Figure 7. *Response of heart rate and blood pressure to methylcholine.* fps^{MF} mice were more sensitive to methylcholine induced decreases in heart rate [Panel A: wt (●), fps^{MF} (○); n = 3; p < 0.05(*)]. Decreases in mean arterial pressure was comparable between genotypes. [Panel B: wt (●); fps^{MF} (○); n = 3].

Figure 8. *PDGF-induced tyrosine phosphorylation of Fps in C166 cells.* Global tyrosine phosphorylation responses to increasing concentrations of PDGF in C166 cells and EOMA cells were assessed by anti-pY immunoblotting (Panels A and B, respectively). MFps was activated in a dose dependent manner by PDGF (Panel C, anti-pY blot). Probing the same blots with anti-FpsQE confirms equal loading (Panel C, anti-FpsQE blot). MFps pY activation levels are quantified in Panel F(●). Fer activation was not readily apparent at 1.6 nM PDGF (Panel D), but was slightly visible at 2.4 nM PDGF (Panel E) while Fps was strongly phosphorylated at both concentrations of PDGF (Panel C), suggesting that pY signals were predominantly attributable to Fps.

Figure 9. *MFps but not Fps, was specifically activated by PDGF.* C166 cell lines expressing Myc-epitope-tagged wild type Fps (Fps-Myc) and Myc-epitope-tagged myristoylated Fps (MFps-Myc) were stimulated with PDGF. Myc-tagged variants have higher molecular weights

(approx. 120 kDa) and migrate slower than endogenous Fps (92 kDa) on SDS-PAGE (Panels A, B). Upper blots in each panel represent anti-pY blots, while lower blots represent the same blots after stripping and reprobing with anti-FpsQE to assess loading of either endogenous Fps or Fps-Myc species. The positions of endogenous Fps and Fps-Myc are indicated by arrows. PDGF stimulation of C166-Fps-Myc did not show activation of the Fps-Myc variant (Panel A). This observation was confirmed with anti-Myc IPs (data not shown). As expected endogenous Fps present in these lines was dose-dependently activated by PGDF (Panel A and B; pY blot; lower arrows). Activation of both endogenous and Myc-tagged myristoylated Fps species was observed when C166-Fps^{MF}-Myc cells were stimulated with PDGF (Panel B) suggesting that MFps, but not Fps is specifically sensitized to activation downstream of PDGF.

Figure 10. *MFps but not Fps, is specifically activated by VEGF.* C166 cell lines expressing Myc-epitope-tagged wild type Fps were stimulated with 0-2.4 nM VEGF for 5 min. Dose-dependent tyrosine-phosphorylation of MFps but not Fps was observed (Panel A: pY blot). Blots were stripped and reprobed with anti-FpsQE to confirm loading (Panel A: FpsQE blot). Quantification of the level of activation of MFps with 0-2.4 nM VEGF at 2.5 and 5 min time points are displayed in Panel B. The chart displays transient activation of MFps in response to PDGF. The amplitude of activation appears to increase with time.

Figure 11. *Model of angiogenesis in fps^{MF} mice.* MFps is proposed to alter angiogenesis at 5 points. For details refer to the main text. (Grey, endothelial tubes; textured grey, transformed endothelial tubes; beige, mural coating). STEP 1: MFps promotes Ang-2-mediated vessel destabilization in the genesis stages of angiogenesis. STEP 2: MFps may promote VEGF induced vessel sprouting and branching. STEP 3: Hyper-vessel sprouting and branching as a result of effects intrinsic to the properties of transformed-like endothelial cells in fps^{MF} mice.

STEP 4: Hyper-sensitization of MFps to PDGF signaling may alter normal output from this pathway resulting in pro-angiogenic effects. STEP 5: Abnormal PDGF autocrine signaling as a result of up-regulation of PDGFR expression may contribute to increased vessel sprouting and branching.

References

1. Carmeliet P: Mechanisms of angiogenesis and arteriogenesis. Nat Med 2000, 6:389-395
2. Yancopoulos GD, Davis S, Gale NW, Rudge JS, Wiegand SJ, Holash J: Vascular-specific growth factors and blood vessel formation. Nature 2000, 407:242-248
3. Betsholtz C, Karlsson L, Lindahl P: Developmental roles of platelet-derived growth factors. Bioessays 2001, 23:494-507
4. Folkman J, D'Amore PA: Blood vessel formation: what is its molecular basis? Cell 1996, 87:1153-1155
5. Davidson JM, Aquino AM, Woodward SC, Wilfinger WW: Sustained microgravity reduces intrinsic wound healing and growth factor responses in the rat. Faseb J 1999, 13:325-329
6. Risau W, Drexler H, Mironov V, Smits A, Siegbahn A, Funa K, Heldin CH: Platelet-derived growth factor is angiogenic in vivo. Growth Factors 1992, 7:261-266
7. Sano H, Sudo T, Yokode M, Murayama T, Kataoka H, Takakura N, Nishikawa S, Nishikawa SI, Kita T: Functional blockade of platelet-derived growth factor receptor-beta but not of receptor-alpha prevents vascular smooth muscle cell accumulation in fibrous cap lesions in apolipoprotein E-deficient mice. Circulation 2001, 103:2955-2960
8. Sano H, Ueda Y, Takakura N, Takemura G, Doi T, Kataoka H, Murayama T, Xu Y, Sudo T, Nishikawa S, Fujiwara H, Kita T, Yokode M: Blockade of platelet-derived growth factor receptor-beta pathway induces apoptosis of vascular endothelial cells and disrupts glomerular capillary formation in neonatal mice. Am J Pathol 2002, 161:135-143
9. Heldin CH, Ostman A, Ronnstrand L: Signal transduction via platelet-derived growth factor receptors. Biochim Biophys Acta 1998, 1378:F79-113
10. Heldin CH, Westermark B: Mechanism of action and in vivo role of platelet-derived growth factor. Physiol Rev 1999, 79:1283-1316
11. Kim HR, Upadhyay S, Korsmeyer S, Deuel TF: Platelet-derived growth factor (PDGF) B and A homodimers transform murine fibroblasts depending on the genetic background of the cell. J Biol Chem 1994, 269:30604-30608
12. Hellstrom M, Gerhardt H, Kalen M, Li X, Eriksson U, Wolburg H, Betsholtz C: Lack of pericytes leads to endothelial hyperplasia and abnormal vascular morphogenesis. J Cell Biol 2001, 153:543-553
13. Hellstrom M, Kal n M, Lindahl P, Abramsson A, Betsholtz C: Role of PDGF-B and PDGFR-beta in recruitment of vascular smooth muscle cells and pericytes during embryonic blood vessel formation in the mouse. Development 1999, 126:3047-3055.
14. Lindahl P, Johansson BR, Leveen P, Betsholtz C: Pericyte loss and microaneurysm formation in PDGF-B-deficient mice. Science 1997, 277:242-245
15. Leveen P, Pekny M, Gebre-Medhin S, Swolin B, Larsson E, Betsholtz C: Mice deficient for PDGF B show renal, cardiovascular, and hematological abnormalities. Genes Dev 1994, 8:1875-1887
16. Soriano P: Abnormal kidney development and hematological disorders in PDGF beta-receptor mutant mice. Genes Dev 1994, 8:1888-1896
17. Lindahl P, Hellstrom M, Kalen M, Karlsson L, Pekny M, Pekna M, Soriano P, Betsholtz C: Paracrine PDGF-B/PDGF-Rbeta signaling controls mesangial cell development in kidney glomeruli. Development 1998, 125:3313-3322

18. Greer PA: Closing in on the biological functions of Fps/Fes and Fer. Nature Reviews Molecular Cell Biology 2002, 3:278-289

19. Aspenstrom P: A Cdc42 target protein with homology to the non-kinase domain of FER has a potential role in regulating the actin cytoskeleton. Curr Biol 1997, 7:479-487.

20. Haigh J, McVeigh J, Greer P: The fps/fes tyrosine kinase is expressed in myeloid, vascular endothelial, epithelial, and neuronal cells and is localized in the trans-golgi network. Cell Growth Differ 1996, 7:931-944.

21. Senis YA, Sangrar W, Zirngibl RA, Craig AWB, Lee DH, Greer PA: Fps/Fes and Fer Nonreceptor Protein-Tyrosine Kinases Regulate Collagen- and ADP-Induced Platelet Aggregation. J Cell Biol 2002

22. Sangrar W: Transgenic Mice Expressing an Activated Mutant Fps/Fes nonreceptor Protein-Tyrosine kinase are Characterized by Bleeding Defects, Thrombocytopenia and Increased Platelet Volume. J Cell Biol 2002

23. Senis Y, Zirngibl R, McVeigh J, Haman A, Hoang T, Greer PA: Targeted disruption of the murine fps/fes proto-oncogene reveals that Fps/Fes kinase activity is dispensable for hematopoiesis. Mol Cell Biol 1999, 19:7436-7446.

24. Zirngibl RA, Senis Y, Greer PA: Enhanced endotoxin-sensitivity in Fps/Fes-null mice with minimal defects in hematopoietic homeostasis. Mol Cell Biol 2002, 22:2472-2486

25. Hackenmiller R, Kim J, Feldman RA, Simon MC: Abnormal Stat activation, hematopoietic homeostasis, and innate immunity in c-fes-/- mice. Immunity 2000, 13:397-407.

26. Yee SP, Mock D, Maltby V, Silver M, Rossant J, Bernstein A, Pawson T: Cardiac and neurological abnormalities in v-fps transgenic mice. Proc Natl Acad Sci U S A 1989, 86:5873-5877.

27. Greer P, Haigh J, Mbamalu G, Khoo W, Bernstein A, Pawson T: The Fps/Fes protein-tyrosine kinase promotes angiogenesis in transgenic mice. Mol Cell Biol 1994, 14:6755-6763.

28. Senis YA, Sangrar W, Zirngibl RA, Craig AWB, Lee DH, Greer PA: Fps/Fes and Fer Nonreceptor Protein-Tyrosine Kinases Regulate Collagen- and ADP-Induced Platelet Aggregation. Journal of Thrombosis and Haemostasis In Press

29. Browder T, Folkman J, Pirie-Shepherd S: The hemostatic system as a regulator of angiogenesis. J Biol Chem 2000, 275:1521-1524

30. Laux V, Seiffge D: Mediator-induced changes in macromolecular permeability in the rat mesenteric microcirculation. Microvasc Res 1995, 49:117-133

31. Levitt RC, Mitzner W: Expression of airway hyperreactivity to acetylcholine as a simple autosomal recessive trait in mice. Faseb J 1988, 2:2605-2608

32. Tse MY, Watson JD, Sarda IR, Flynn TG, Pang SC: Expression of B-type natriuretic peptide in atrial natriuretic peptide gene disrupted mice. Mol Cell Biochem 2001, 219:99-105

33. Wang SJ, Greer P, Auerbach R: Isolation and propagation of yolk-sac-derived endothelial cells from a hypervascular transgenic mouse expressing a gain-of-function fps/fes proto-oncogene. In Vitro Cell Dev Biol Anim 1996, 32:292-299.

34. Craig AW, Greer PA: Fer kinase is required for sustained p38 kinase activation and maximal chemotaxis of activated mast cells. Mol Cell Biol 2002, 22:6363-6374

35. Margolis B, Rhee SG, Felder S, Mervic M, Lyall R, Levitzki A, Ullrich A, Zilberstein A, Schlessinger J: EGF induces tyrosine phosphorylation of phospholipase C-II: a potential mechanism for EGF receptor signaling. Cell 1989, 57:1101-1107

36. Detmar M, Brown LF, Schon MP, Elicker BM, Velasco P, Richard L, Fukumura D, Monsky W, Claffey KP, Jain RK: Increased microvascular density and enhanced leukocyte rolling and adhesion in the skin of VEGF transgenic mice. J Invest Dermatol 1998, 111:1-6

37. Suri C, McClain J, Thurston G, McDonald DM, Zhou H, Oldmixon EH, Sato TN, Yancopoulos GD: Increased vascularization in mice overexpressing angiopoietin-1. Science 1998, 282:468-471

38. Thurston G, Suri C, Smith K, McClain J, Sato TN, Yancopoulos GD, McDonald DM: Leakage-resistant blood vessels in mice transgenically overexpressing angiopoietin-1. Science 1999, 286:2511-2514

39. Thurston G: Complementary actions of VEGF and angiopoietin-1 on blood vessel growth and leakage. J Anat 2002, 200:575-580

40. Thurston G, Rudge JS, Ioffe E, Zhou H, Ross L, Croll SD, Glazer N, Holash J, McDonald DM, Yancopoulos GD: Angiopoietin-1 protects the adult vasculature against plasma leakage. Nat Med 2000, 6:460-463

41. Sato TN, Tozawa Y, Deutsch U, Wolburg-Buchholz K, Fujiwara Y, Gendron-Maguire M, Gridley T, Wolburg H, Risau W, Qin Y: Distinct roles of the receptor tyrosine kinases Tie-1 and Tie-2 in blood vessel formation. Nature 1995, 376:70-74

42. Suri C, Jones PF, Patan S, Bartunkova S, Maisonpierre PC, Davis S, Sato TN, Yancopoulos GD: Requisite role of angiopoietin-1, a ligand for the TIE2 receptor, during embryonic angiogenesis. Cell 1996, 87:1171-1180

43. Andriopoulou P, Navarro P, Zanetti A, Lampugnani MG, Dejana E: Histamine induces tyrosine phosphorylation of endothelial cell-to-cell adherens junctions. Arterioscler Thromb Vasc Biol 1999, 19:2286-2297

44. Silberbach M, Roberts CT, Jr.: Natriuretic peptide signalling: molecular and cellular pathways to growth regulation. Cell Signal 2001, 13:221-231

45. Dhein S, van Koppen CJ, Brodde OE: Muscarinic receptors in the mammalian heart. Pharmacol Res 2001, 44:161-182

46. Brodde OE, Michel MC: Adrenergic and muscarinic receptors in the human heart. Pharmacol Rev 1999, 51:651-690

47. Cines DB, Pollak ES, Buck CA, Loscalzo J, Zimmerman GA, McEver RP, Pober JS, Wick TM, Konkle BA, Schwartz BS, Barnathan ES, McCrae KR, Hug BA, Schmidt AM, Stern DM: Endothelial cells in physiology and in the pathophysiology of vascular disorders. Blood 1998, 91:3527-3561

48. Ferrell JE, Jr., Machleder EM: The biochemical basis of an all-or-none cell fate switch in Xenopus oocytes. Science 1998, 280:895-898

49. Koshland DE, Jr.: The era of pathway quantification. Science 1998, 280:852-853

50. Kim L, Wong TW: The cytoplasmic tyrosine kinase FER is associated with the catenin-like substrate pp120 and is activated by growth factors. Mol Cell Biol 1995, 15:4553-4561.

51. Fong GH, Rossant J, Gertsenstein M, Breitman ML: Role of the Flt-1 receptor tyrosine kinase in regulating the assembly of vascular endothelium. Nature 1995, 376:66-70

52.	Miquerol L, Langille BL, Nagy A: Embryonic development is disrupted by modest increases in vascular endothelial growth factor gene expression. Development 2000, 127:3941-3946

53.	Jones N, Voskas D, Master Z, Sarao R, Jones J, Dumont DJ: Rescue of the early vascular defects in Tek/Tie2 null mice reveals an essential survival function. EMBO Rep 2001, 2:438-445

54.	Hollister AS, Inagami T: Atrial natriuretic factor and hypertension. A review and metaanalysis. Am J Hypertens 1991, 4:850-865

55.	Hirschi KK, D'Amore PA: Pericytes in the microvasculature. Cardiovasc Res 1996, 32:687-698

56.	Lindahl P, Hellstrom M, Kalen M, Betsholtz C: Endothelial-perivascular cell signaling in vascular development: lessons from knockout mice. Curr Opin Lipidol 1998, 9:407-411

57.	Lindahl P, Bostrom H, Karlsson L, Hellstrom M, Kalen M, Betsholtz C: Role of platelet-derived growth factors in angiogenesis and alveogenesis. Curr Top Pathol 1999, 93:27-33

58.	Morikawa S, Baluk P, Kaidoh T, Haskell A, Jain RK, McDonald DM: Abnormalities in pericytes on blood vessels and endothelial sprouts in tumors. Am J Pathol 2002, 160:985-1000

59.	Arregui C, Pathre P, Lilien J, Balsamo J: The nonreceptor tyrosine kinase fer mediates cross-talk between N- cadherin and beta1-integrins. J Cell Biol 2000, 149:1263-1274.

60.	Piedra J, Miravet S, Castano J, Palmer HG, Heisterkamp N, Garcia de Herreros A, Dunach M: p120 Catenin-associated Fer and Fyn tyrosine kinases regulate beta-catenin Tyr-142 phosphorylation and beta-catenin-alpha-catenin Interaction. Mol Cell Biol 2003, 23:2287-2297

61.	Xu G, Craig AW, Greer PA, Miller M, Anastasiades P, Lilien J, Balsamo J: Continuous coupling of cadherin to the cytoskeleton requires phosphorylation of PTP1B by Fer. (Submitted)

62.	Carmeliet P, Lampugnani MG, Moons L, Breviario F, Compernolle V, Bono F, Balconi G, Spagnuolo R, Oostuyse B, Dewerchin M, Zanetti A, Angellilo A, Mattot V, Nuyens D, Lutgens E, Clotman F, de Ruiter MC, Gittenberger-de Groot A, Poelmann R, Lupu F, Herbert JM, Collen D, Dejana E: Targeted deficiency or cytosolic truncation of the VE-cadherin gene in mice impairs VEGF-mediated endothelial survival and angiogenesis. Cell 1999, 98:147-157

63.	Carmeliet P: Developmental biology. One cell, two fates. Nature 2000, 408:43, 45

64.	Mochizuki Y, Nakamura T, Kanetake H, Kanda S: Angiopoietin 2 stimulates migration and tube-like structure formation of murine brain capillary endothelial cells through c-Fes and c-Fyn. J Cell Sci 2002, 115:175-183

65.	Moyon D, Pardanaud L, Yuan L, Breant C, Eichmann A: Selective expression of angiopoietin 1 and 2 in mesenchymal cells surrounding veins and arteries of the avian embryo. Mech Dev 2001, 106:133-136

66.	Holmgren L, Glaser A, Pfeifer-Ohlsson S, Ohlsson R: Angiogenesis during human extraembryonic development involves the spatiotemporal control of PDGF ligand and receptor gene expression. Development 1991, 113:749-754

67.	Kolibaba KS, Druker BJ: Protein tyrosine kinases and cancer. Biochim Biophys Acta 1997, 1333:F217-248

68. Fleming TP, Saxena A, Clark WC, Robertson JT, Oldfield EH, Aaronson SA, Ali IU: Amplification and/or overexpression of platelet-derived growth factor receptors and epidermal growth factor receptor in human glial tumors. Cancer Res 1992, 52:4550-4553

69. Hermanson M, Funa K, Hartman M, Claesson-Welsh L, Heldin CH, Westermark B, Nister M: Platelet-derived growth factor and its receptors in human glioma tissue: expression of messenger RNA and protein suggests the presence of autocrine and paracrine loops. Cancer Res 1992, 52:3213-3219

70. Fleming TP, Matsui T, Aaronson SA: Platelet-derived growth factor (PDGF) receptor activation in cell transformation and human malignancy. Exp Gerontol 1992, 27:523-532

71. Leon SP, Zhu J, Black PM: Genetic aberrations in human brain tumors. Neurosurgery 1994, 34:708-722

72. Carmeliet P, Ferreira V, Breier G, Pollefeyt S, Kieckens L, Gertsenstein M, Fahrig M, Vandenhoeck A, Harpal K, Eberhardt C, Declercq C, Pawling J, Moons L, Collen D, Risau W, Nagy A: Abnormal blood vessel development and lethality in embryos lacking a single VEGF allele. Nature 1996, 380:435-439

73. Cristofanilli M, Charnsangavej C, Hortobagyi GN: Angiogenesis modulation in cancer research: novel clinical approaches. Nat Rev Drug Discov 2002, 1:415-426

74. Nygren P, Larsson R: Overview of the clinical efficacy of investigational anticancer drugs. J Intern Med 2003, 253:46-75

The *fps/fes* Proto-Oncogene Regulates Hematopoietic Lineage Output

Waheed Sangrar[1], Yan Gao[1], Ralph A. Zirngibl[1,2], Michelle L. Scott[1,2] and Peter A. Greer[1,3]*

[1] Division of Cancer Biology and Genetics, Queen's University Cancer Research institute, Kingston, Ontario, K7L 3N6, Canada

[2] Department of Biochemistry, Queen's University, Kingston, Ontario, K7L 3N6 Canada

[3] Department of Pathology, Queen's University, Kingston, Ontario, K7L 3N6, Canada

*To whom correspondence should be addressed: Peter A. Greer, Department of Pathology, Division of Cancer Biology and Genetics, Cancer Research Institute, Botterell Hall, Room A309, Queen's University, Kingston, Ontario, K7L 3N6, Canada. Tel: (613) 533-2813; FAX: (613) 533-6830; email: greerp@post.queensu.ca.

General Hematopoiesis

<u>Word Count</u>

Abstract: 222

Total: 3992

Abstract

Objective. The *fps/fes* proto-oncogene is abundantly expressed in myeloid cells, and the Fps/Fes cytoplasmic protein-tyrosine kinase is implicated in signaling downstream from hematopoietic cytokines, including interleukin 3 (IL-3), granulocyte-macrophage colony stimulated factor (GM-CSF) and erythropoietin (Epo). Studies using leukemic cell lines have previously suggested that Fps/Fes contributes to granulomonocytic differentiation, and that it might play a more selective role in promoting survival and differentiation along the monocytic pathway. In this study we have utilized transgenic mice (fps^{MF} mice) tissue-specifically expressing an activated Fps/Fes kinase to investigate the role of this kinase in hematopoiesis.

Methods. Hematopoietic function in *wild type* and fps^{MF} mice was assessed using lineage analysis, hematopoietic progenitor cell-colony forming assays and biochemical approaches.

Results. We show that transgenic mice tissue-specifically expressing an activated Fps/Fes kinase displayed a skewed hematopoietic output. These mice had increased numbers of circulating granulocytic and monocytic cells and a corresponding decrease in lymphoid cells. Bone marrow colony assays of progenitor cells revealed a significant increase in the number of both granulomonocytic and multi-lineage progenitors. A molecular analysis of signaling in mature monocytic cells showed that activated Fps/Fes promoted GM-CSF induced STAT3, STAT5 and ERK1/2 activation.

Conclusions. These observations support a role for Fps/Fes in signaling pathways that contribute to lineage determination at the level of multi-lineage hematopoietic progenitors as well as the more committed granulomonocytic progenitors.

2

Introduction

The *fps/fes* proto-oncogene (here after called *fps*) encodes a cytoplasmic protein-tyrosine kinase that is abundantly expressed in cells of the hematopoietic lineage [1]. Although the precise molecular role for the Fps kinase is not understood, it has been implicated in signaling downstream from a number of hematopoietic cytokines including IL-3 [2], IL-4 [3,4], GM-CSF [2,5], Epo [6,7] and IL-6 [8]. In some cases, a link to PI3' kinase and cell survival has been made [3,4]; and in other studies a connection with activation of signal transducers and activators of transcription (STATs) has been demonstrated [5,6,9-11] which would have implications in both survival and differentiation.

In early studies of *fps*, forced expression in the K562 human erythroleukemic cell line correlated with myeloid differentiation potential [12], and antisense blocking experiments suggested that Fps protects human leukemic HL60 or fresh acute promyelocytic leukemia blast cells from programmed cell death during induced granulocytic, but not monocytic differentiation [13,14]. Transduction of the human bipotential promonocytic leukemic cell line U937 with retrovirus encoding an activated form of Fps was shown to drive differentiation down the monocytic pathway [15]. Interestingly, this appeared to occur at the expense of granulocytic differentiation, and it correlated with enhanced activity of the *ets* family transcriptional regulator, PU.1 [15]. More recently, the same activated Fps-encoding retrovirus promoted survival and granulocytic differentiation of the IL-3 dependent 32D cell line, and this correlated with activation of the transcription factors C/EBPα and STAT3 [16]. These observations suggested that Fps might participate in lineage determining signaling pathways involving PU.1, C/EBPα and STAT3 that govern the survival and differentiation of granulomonocytic progenitors.

Cell culture based experiments like those described above suggested that loss of *fps* would seriously compromise *in vivo* myelopoiesis. This hypothesis has recently been addressed by gene targeting in transgenic mice. A mouse knock-in mutation that abolished Fps kinase activity without compromising its expression, resulted in only a mild defect in cytokine-induced STAT activation in myeloid cells, and there were no detectable defects in myelopoiesis in these *fps*[KR/KR] mice [11]. Surprisingly different phenotypes have since been reported in mice strains targeted with null mutations. In one case enhanced myelopoiesis was reported in *fps*-null mice; and this correlated with increased GM-CSF and IL-6 induced STAT3 and STAT5 activation in cultured myeloid cells [17]. This prompted an interesting model where Fps was hypothesized to compete with Jak2 kinase for access to STAT 3 or STAT5 [17]. However, an independently generated *fps*-null mouse strain displayed no obvious defect in cytokine induced STAT3 or STAT5 activation [18]. Furthermore, a decrease in circulating granulocytes and monocytes from this *fps*^{-/-} mouse strain was observed; and this phenotype was corrected by a *fps* transgene in *fps*[-/-;Tg] mice [18]. These observations were consistent with the phenotypes observed earlier in *fps*[KR/KR] mice, and in the earlier cell culture experiments. Furthermore, they supported the hypothesis that Fps does participate in myelopoiesis, but that its function might be partially redundant with other kinases, such as members of the Jak, Src or Syk families, or perhaps the Fps-related Fer kinase [19]. It follows that while myelopoiesis might not be seriously compromised in Fps-deficient mice, it might be enhanced in mice expressing an activated Fps kinase. We have now examined myelopoiesis in a strain of transgenic mice which were engineered to express a gain-of-function mutant Fps kinase in a tissue-specific fashion [20]. The addition of five amino acids immediately after the amino-terminal glycine in Fps created a minimal Src-like myristoylation consensus sequence. This MFps protein is efficiently myristoylated, and this provided weak

4

transforming activity in rat fibroblasts [20]. The complete human *fps* locus including this mutation was used to generate *fps^{MF}* transgenic mice which tissue-specifically expressed the active MFps kinase.

In the present study, we show that *in vivo* expression of activated MFps correlated with a skewing of hematopoiesis, manifested by increased granulomonocytic output and a corresponding decrease in lymphoid cells. Increased numbers of granulomonocytic precursors were detected in the bone marrow using flow cytometry-based lineage analysis and progenitor colony assays. Interestingly, there was also evidence of decreased B-cell progenitors in the bone marrow and a block in T-cell maturation. Bone marrow derived monocytes from *fps^{MF}* mice displayed enhanced GM-CSF induced activation of STAT3, STAT5, and ERK. Based upon these observations, we propose a molecular model for Fps involvement in cytokine signaling which is consistent with phenotypes seen in all of our transgenic mouse strains. Furthermore, we propose a role for Fps in regulating lineage determination by multipotential hematopoietic progenitors.

Experimental Procedures

Mice

Derivation of fps^{MF} transgenic mice, expressing myristoylated MFps were previously described [20]. The fps^{MF} line is maintained in an out-bred CD-1 background and is housed at the Animal Care Facility at Queen's University, Kingston, ON Canada. All protocols involving animals were approved by the institutional animal care committee in accordance with the guidelines of the Canadian Council on Animal Care.

Peripheral white blood cell analysis

Whole blood was acquired by cardiac puncture as previously described [18].

Flow cytometry

Bone marrow (from femur), spleen, and thymi were obtained from *wt* and fps^{MF} mice and single cell suspensions were prepared for flow cytometry as previously described [11,18]. Cells were incubated with either phycoerythrin (PE) or fluorescein isothiocyanate (FITC) conjugated monoclonal antibodies (Pharmingen Canada unless otherwise specified). Bone marrow cells and splenocytes were incubated with either PE–Ly6G and FITC-CD11b or with PE-CD45R/B220 and FITC-IgM (Serotec). Splenocytes were also incubated with PE-CD8 (Leinco Technologies, Inc) and FITC-CD4 (Leinco Technologies, Inc).

Cell colony assays

Methylcellulose progenitor assays were performed as previously described [11]. Methylcellulose was supplemented with two different cocktails of recombinant cytokines (R&D Systems, Minneapolis, MN): One cocktail consisted of 50 ng/ml Steel factor (SF), 5 ng/ml IL-3, 10 ng/ml IL-6, 10 ng/ml Tpo, 1 U/ml Epo and 5 ng/ml GM-CSF and the second cocktail consisted of 1 U/ml Epo and 5 ng/ml GM-CSF.

GM-CSF stimulation of bone-marrow cultures

Bone marrow-derived macrophage were prepared, cultured and stimulated with recombinant cytokine as previously described [11]. Stimulations were carried out with 25 ng/ml recombinant GM-CSF (0-30 min) (R&D Systems) and soluble cell lysates were prepared for subsequent immunoblotting analysis [11]. Lysates were quantified using a BioRad protein assay kit (BioRad) and equal masses of total protein were utilized for Western blotting analyses. Blots were probed with the following antibodies according to manufacturer instructions: Fps/Fer (FpsQE) [21], phospho-(p)STAT3, STAT3, pSTAT5A/B, STAT5A, pJAK2, JAK2, ERK1/2 (all from Upstate Biotechnology); pp38, pAKT, AKT (all from Cell Signaling technologies); p38, pERK1/2, and pTyr (clone PY99) mAb (all from Santa Cruz Biotechnologies). In some instances, SDS-PAGE gels were directly stained with Sypro Ruby Protein fluorescent gel stain (Molecular Probes) in order to confirm equal loading of total protein.

Statistical analysis

Student t-tests and means were determined using Microsoft Excel (Microsoft, Canada) and GraphPad Prism statistical analysis software (GraphPad Software Inc, San Diego, CA). t-test analyses of data sets with p-values ≤ 0.05 were considered statistically significant. Where appropriate, data are expressed as mean $\pm$ SEM.

Results

Elevated levels of circulating monocytes and granulocytes in fps^MF mice

Fps is highly expressed in myeloid cells and has been implicated in terminal differentiation and survival of myeloid progenitors, suggesting that perturbations in the function of this kinase might affect hematopoietic output. Consistent with this hypothesis, peripheral blood white cell differentials were markedly abnormal in the *fps^MF* transgenic mice. This was reflected by elevations in percentages and absolute levels of circulating neutrophils, monocytes and basophils; and in contrast, by decreased lymphocytes (Table 1). Indeed, the percentage decrease in lymphocytes closely corresponded to the increase in the percentage of granulomonocytic cells. Perturbations of this extent were not observed in a transgenic line over-expressing a wild type human *fps* transgene Fps [18] suggesting that the abnormal white blood cell outputs in *fps^MF* mice were not due to Fps over-expression, but were linked to expression of the activated MFps kinase. Interestingly, *fps^MF* mice also displayed decreases in erythroid output (Table 1) and the opposite was observed in *fps^-/-* mice [18]. Taken together these observations suggested that expression of MFps might skew hematopoietic output towards the granulomonocytic lineage at the expense of both the erythroid and lymphoid lineages. This would be consistent with a contributing role for Fps in the regulation of hematopoietic lineage determination by committed multipotential hematopoietic progenitor cells.

Perturbations in undifferentiated myeloid progenitors and mature B-cells in fps^MF mice

Lineage analyses of bone marrow cells from *fps^-/-* mice had previously shown a statistically significant reduction in Ly-6G+/CD11b+ granulomonocytic cells; and this was rescued by a human *fps* transgene [18]. This was consistent with a positive role for Fps in maturation of granulomonocytic cells in the bone marrow, and suggested that activated Fps might therefore

8

enhance granulomonocytic output. While fps^{MF} mice did not display the expected increase in Ly-6G+/CD11b+ bone marrow cells, there was a statistically significant increase in presumptive granulomonocytic progenitor Ly6-G⁻/CD11b⁺ cells in both bone marrow and spleen (Fig. 1 and 2). These observations correlated with the peripheral blood data depicting increased granulocyte and monocyte output (Table 1). We also observed statistically significant decreases in mature B-cell populations (B220⁺IgM⁺) in the bone marrow of fps^{MF} mice (Fig. 1); and this correlated with the reduced output of lymphocytes in the periphery (Table 1). However, no differences were observed in mature B-cell levels in the spleens of fps^{MF} mice (Fig. 2).

Increases in bone marrow CFU-GM and CFU-GEMM colonies in fps^{MF} mice

In order to confirm that increases in granulomonocytic output are a result of abnormal hematopoiesis, we performed methylcellulose colony assays to assess the number of bone marrow progenitor cells in *wt* and fps^{MF} mice. These assays were performed using either a cocktail of hematopoietic factors (condition A: Scf, GM-CSF, Epo, Tpo, IL-6, IL-3), or a more restricted condition (condition B: Epo and GM-CSF). In condition A, fps^{MF} CFU-GM colonies were increased 1.8 fold ($p = 0.014$) relative to *wt*, while the numbers of other mixed colonies were normal (Fig. 3A). A comparable fold increase of CFU-GM colonies was observed in the more limited cytokine condition B (1.5-fold increase; $p = 0.069$) (Fig. 3B). We also observed a 1.9-fold increase ($p = 0.0281$) in CFU-GEMM mixed colonies in condition B, but the numbers of CFU-GEMM colonies were the same in condition A. These results indicated a selectively enhanced GM-CSF responsiveness of fps^{MF} multi-lineage progenitors cells.

Evidence for T-cell maturation defects in fps^{MF} mice

Splenocytes from transgene-rescued Fps-null mice ($fps^{-/-:Tg}$), which over-express wild type Fps, were previously shown to have slight decreases in the CD4 and CD8 single-positive populations

[18]. This led us to examine these populations in the spleens and thymi of fps^{MF} mice. Statistically significant decreases of both CD4$^+$CD8$^-$ and CD4$^-$CD8$^+$ cells were apparent in the spleen of fps^{MF} mice (Fig 4, C and D). Statistically significant increases in CD4$^+$CD8$^-$ populations were seen the thymi of fps^{MF} mice (Fig. 4, A and B). These data were consistent with the observed decreases of lymphocytes in the periphery in fps^{MF} mice, and suggested a role for Fps in regulating the development and/or maturation of T-cells.

Enhanced cytokine-induced STAT3, STAT5 and ERK activation in fps^{MF} macrophages

Given the apparent evidence for enhanced myelopoiesis in fps^{MF} mice we next examined expression of Fps and MFps in bone marrow derived macrophages, and cytokine induced activation of Jak2 kinase, STAT3/5, ERK1/2 and other signaling proteins. Western blotting analysis confirmed that MFps is over-expressed in macrophages from fps^{MF} mice relative to endogenous Fps (Fig. 5). The relative levels of MFps and Fps in macrophage cultures was consistent with the previously characterized tissue-specific expression of the fps^{MF} transgene, and the estimated ten transgene copies relative to two endogenous *fps* alleles [20]. The fatty acid modification resulted in MFps migrating between p94Fer and p92Fps (Fig. 5).

An examination of signaling in bone marrow macrophages from fps^{MF} mice revealed increased STAT3 and STAT5A/B phosphorylation in response to GM-CSF (Fig. 5). Although the degree of enhanced STAT activation was not dramatic, this was consistently observed in three independent experiments. These results suggested a positive effect of Fps on STAT signaling downstream of GM-CSF and further suggested that MFps promoted a higher degree of STAT activation. Equal loading was confirmed using antibodies specific for Fps/Fer, STAT3, STAT5A/B and total protein levels (Fig. 5). Interestingly, there were no differences in the

10

kinetics of activation of JAK2 between *wt* and fps^{MF} mice, suggesting that Fps affected STAT signaling in a JAK2 independent fashion.

Since the degree of enhanced STAT activation in fps^{MF} macrophages was modest, we also examined the kinetics of GM-CSF induced activation of several other downstream effectors (Figure 6). We were unable to observe significant differences in the kinetics of activation of p38, AKT, and JNK (Fig. 6 and data not shown). However, we frequently observed increases in the kinetics of ERK1/2 activation (Fig. 6).

Discussion

Although *fps* and *fes* were first identified as retroviral oncogenes capable of causing sarcomas in chickens and cats, respectively, an involvement of the cellular *fps/fes* proto-oncogene in malignancy has not yet been determined. Mutations in *fps/fes* have recently been reported in human colon carcinoma [22]; however, the involvement of these in disease progression was not explored. The oncogenic potential of *fps/fes* was explored in an early transgenic mouse model by expressing a retroviral Gag-Fps protein under the control of a minimal β-globin promoter [23,24]. These mice developed a range of tumors that were likely determined in large part by the tissue distribution of transgene expression achieved in the specific founder lines. The complete human *fps* locus was next used to generate transgenic mice with tissue-specific over-expression of Fps [25]. The expected high level of myeloid transgene expression was achieved, but no myeloid leukemia or other malignancies were observed; and no hematopoietic defects were observed.

Retroviral Gag is thought to contribute to activation of Fps by enhancing oligomerization and association with the membrane, and cellular Fps is thought to contribute to cytokine receptor signaling, perhaps through phosphorylation of the receptors or associated signaling molecules. We therefore attempted to generate a weaker gain-of-function mutant *fps* allele by introducing coding sequences for amino terminal myristoylation into the context of a genomic *fps* transgene [20]. Our rationale was that myristoylated Fps (MFps) would associate constitutively with lipid bilayers, thereby enhancing interactions with integral membrane proteins, including cytokine receptors. We reasoned that this might lead to Fps-mediated phosphorylation and activation of cytokine receptors or downstream effectors in the presence of sub-threshold levels of ligands. Transgenic mice expressing this *fps^{MF}* allele were generated and shown to over-express MFps in

a tissue-specific fashion [20]. The fps^{MF} mice have a number of interesting phenotypes that have helped to uncover previously unsuspected biological roles for Fps in the regulation of angiogenesis [20], and thrombosis [18]. However, although a high level of MFps expression was observed in the myeloid lineages, we did not observe any myeloid leukemias in these animals. We now report a hematopoietic phenotype in fps^{MF} mice that implicates Fps in the regulation of hematopoietic lineage determination by multi-potential progenitor cells; a role which might extend to the pluripotential hematopoietic stem cell.

Previous studies using cultured human leukemic cell lines which retain the ability to differentiate have suggested that Fps might preferentially drive hematopoietic commitment along the monocytic lineage [15], and that it might be essential for survival during monocytic, but not granulocytic differentiation [13,14]. A more recent study using the factor dependent 32D myeloid leukemic cell line suggested that activated Fps can also promote survival and granulocytic differentiation [26]. Analysis of peripheral blood cell composition provided initial evidence for enhanced myeloid output in the fps^{MF} mice (Table 1). This also pointed to a role for Fps in myelopoiesis, but it did not support a more selective monocytic role, because statistically significant increases were seen in circulating neutrophils, basophils and monocytes. Furthermore, this effect on myeloid cell output was underscored by the apparent increase in total circulating white blood cells, even though lymphocytes, which represent the majority of circulating white blood cells, were actually decreased by approximately 10% in the fps^{MF} mice. This suggested that Fps might be exerting an affect higher up in the hematopoietic differentiation hierarchy.

In order to determine the level in the hematopoietic differentiation hierarchy where MFps was acting to cause this apparent skewing in lineage output, we attempted to trace these

13

differences back to hematopoietic tissues. Lineage analysis of bone marrow cells revealed statistically significant increases in the presumptive granulomonocytic progenitor pools (Ly6-G⁻ CD11b⁺) in the bone marrow (Fig. 1); and a similar increase in this population was noted in the spleen (Fig. 2). Mature B-cell levels were also reduced in the bone marrow (Fig. 1). These observations are consistent with the hypothesis that Fps was acting on an earlier multi-potential progenitor and driving its differentiation toward the myeloid lineages at the expense of the lymphoid lineages. Further analysis using progenitor cell colony assays clearly demonstrated an increase in CFU-GM granulomonocytic progenitor cells in the bone marrow (Fig. 3); and interestingly, multi-lineage CFU-GEMM colonies were also significantly higher in response to GM-CSF plus Epo, but not to a more extensive cytokine cocktail (Scf, GM-CSF, Epo, Tpo, IL-6, IL-3). These observations suggested that activated Fps was promoting an increase in granulomonocytic progenitors in the bone marrow. However, they did not indicate that this effect extended to more committed monocytic progenitors since the number of CFU-M was not higher in either cytokine condition.

Our observations support the hypothesis that MFps promotes the expansion of multi-lineage progenitors as well as bipotential granulomonocytic progenitors in the bone marrow, but that this effect does not extend to the more committed myelomonocytic progenitors. This would suggest that Fps is expressed in multi-lineage progenitors, and perhaps even in hematopoietic stem cells. In support of this, a *fps*-directed Cre transgene achieved deletion of a loxP flanked PIGA gene in all hematopoietic lineages, including lymphoid cells [27]. Furthermore, bone marrow from these compound transgenic mice established PIGA-deficient long term hematopoietic repopulation potential [27]. Those observations are consistent with Fps being expressed in the pluripotent hematopoietic stem cell. It remains to be determined if Fps might actually play a significant

biological role in the hematopoietic stem cell. This will require isolation and characterization of these cells using hematopoietic reconstitution methods.

While we did not attempt to directly measure lymphoid progenitors, lineage analysis of bone marrow with B-cell markers (B220 and IgM) revealed a statistically significant decrease in the double positive mature B-cells (Fig. 1). Similar analysis of T-cells in the spleen showed a decrease in both CD4 and CD8 single positive populations (Fig. 4). However, in the thymus, we observed a reduction in the number of double positive cells that was accompanied with an interesting increase in the single positive populations. While these observations are consistent with the reduced T-cell output seen in the fps^{MF} mice, they also suggested a potential defect in maturation of T-cell progenitors. To our knowledge, there are no published reports suggesting a role for Fps in lymphopoiesis. However, we have recently observed lymphopoiesis defects in mice targeted with kinase-inactivating mutations in both Fps and Fer (unpublished data, 2002). It will be interesting to explore whether Fps expression is intrinsic to T-cells and contributes to their ontogeny; or alternatively, if Fps expression in supporting stromal cells might provide important extrinsic signals to developing T-cells.

Analysis of transgenic and gene targeted mice are revealing an even wider role for Fps and the related Fer kinase in the regulation of hematopoiesis and the function of mature cells. For example, a role for Fps and Fer in GPVI collagen receptor signaling in platelets has recently been described [28] and mice targeted with kinase-inactivating mutations in both Fps and Fer display hematopoietic defects that are consistent with a redundant role for these kinases in regulation of hematopoiesis [19]. Thus, Fps and Fer may play biologically significant regulatory roles in hematopoietic lineage-determination by the earliest uncommitted progenitors, and also by more committed progenitors. In line with this latter possibility, expression of activated Fps

(MFps) appears to drive progenitors at several levels toward the granulomonocytic pathway, and this might occur at the expense of lymphoid, erythroid and megarkaryotic lineages (Figure 7). The molecular basis of this hypothetical effect however, remains to be determined and will require the characterization of signaling events in highly enriched preparations of progenitor cells.

A role for Fps in downstream signaling from cytokine receptors in myeloid cells is supported by a number of studies using leukemic cell lines or peripheral while blood cells. We examined signaling in bone marrow derived macrophages from mice targeted with a kinase-inactivating knock-in mutation ($fps^{KR/KR}$). In $fps^{KR/KR}$ macrophages, we reported subtle reductions in both cytokine-induced STAT activation and lipopolysaccharide induced ERK activation [11]. Others subsequently reported a striking enhancement of cytokine-induced STAT activation in macrophages from a Fps-knockout model [17]. This lead to an attractive model suggesting Fps and JAK2 compete with one another for access to STAT downstream of cytokine-activated receptors. Accordingly, while Fps might be capable of STAT phosphorylation, it would not be as effective as JAK2 in this role, and would thus serve to attenuate STAT activation by JAK2. This model predicted that kinase-dead Fps would be an even more effective inhibitor of JAK2-mediated STAT activation. However, in the complete absence of Fps, JAK2 would be unrestrained, leading to hyperactivation of STAT. This model was consistent with results from $fps^{KR/KR}$ mice [11] and the $fps^{-/-}$ mice described by those investigators [17]. However, we have since generated an independent line of $fps^{-/-}$ mice which did not display cytokine-induced hyperactivation of STAT [18]. We have now further complemented our *in vivo* analysis of Fps/STAT signaling using macrophages from the fps^{MF} mice. Slightly enhanced GM-CSF induced STAT3, STAT5, and ERK1/2 phosphorylation was

16

observed in bone marrow derived macrophages from these *fps^MF* mice. JAK2 activation was not affected, nor was that of p38 or JNK. These observations further support a direct role for Fps in phosphorylation of STAT. However, our combined genetic mouse models are not consistent with a role for Fps in attenuation of STAT phosphorylation by JAK2. We propose an alternative model whereby Fps, JAK2, SYK- and SRC-family kinases could all contribute to STAT phosphorylation at the activated cytokine receptor (Fig. 8). JAK2 would be the major player; but SYK, LYN and perhaps other related kinases, as well as Fps and perhaps Fer, could also contribute. Fps might participate by directly phosphorylating STAT, but it might also contribute to STAT activation by phosphorylation of the receptor, or perhaps serve a scaffolding role. According to this model, slightly enhanced or diminished STAT phosphorylation could occur in the presence of MFps or kinase-dead Fps, respectively. But in the complete absence of Fps, JAK2, LYN or other kinases could compensate, making it difficult to observe any obvious reduction in STAT activation. We cannot exclude the possibility that Fps might play a more dominant regulatory role in cytokine signaling under specific cell culture conditions, and this could explain the differences seen by other investigators using a different Fps-null strain of mice [17]. However, we have never observed hyperactivation of STAT in any primary cells from our *fps^{-/-}* mice, and in some circumstances we observed reduced activation of STAT, as well as other signaling molecules. We expect that a careful analysis of cytokine and other signaling pathways in myeloid cells from different tissue sources and at different stages of maturation and activation from our panel of Fps transgenic models will help to unravel this confusion. Clearly additional biochemical characterization will be required before we have a complete understanding of the molecular function of the Fps kinase in cell signaling.

Acknowledgements

References

1. Greer PA (2002) Closing in on the biological functions of Fps/Fes and Fer. Nature Reviews Molecular Cell Biology 3:278

2. Hanazono Y, Chiba S, Sasaki K, Mano H, Miyajima A, Arai K, Yazaki Y, Hirai H (1993) c-fps/fes protein-tyrosine kinase is implicated in a signaling pathway triggered by granulocyte-macrophage colony-stimulating factor and interleukin-3. Embo J 12:1641

3. Izuhara K, Feldman RA, Greer P, Harada N (1996) Interleukin-4 induces association of the c-fes proto-oncogene product with phosphatidylinositol-3 kinase. Blood 88:3910

4. Jiang H, Foltenyi K, Kashiwada M, Donahue L, Vuong B, Hehn B, Rothman P (2001) Fes mediates the IL-4 activation of insulin receptor substrate-2 and cellular proliferation. J Immunol 166:2627

5. Brizzi MF, Aronica MG, Rosso A, Bagnara GP, Yarden Y, Pegoraro L (1996) Granulocyte-macrophage colony-stimulating factor stimulates JAK2 signaling pathway and rapidly activates p93fes, STAT1 p91, and STAT3 p92 in polymorphonuclear leukocytes. J Biol Chem 271:3562

6. Kirito K, Nakajima K, Watanabe T, Uchida M, Tanaka M, Ozawa K, Komatsu N (2002) Identification of the human erythropoietin receptor region required for Stat1 and Stat3 activation. Blood 99:102

7. Hanazono Y, Chiba S, Sasaki K, Mano H, Yazaki Y, Hirai H (1993) Erythropoietin induces tyrosine phosphorylation and kinase activity of the c-fps/fes proto-oncogene product in human erythropoietin-responsive cells. Blood 81:3193

8. Matsuda T, Fukada T, Takahashi-Tezuka M, Okuyama Y, Fujitani Y, Hanazono Y, Hirai H, Hirano T (1995) Activation of Fes tyrosine kinase by gp130, an interleukin-6 family cytokine signal transducer, and their association. J Biol Chem 270:11037

9. Nelson KL, Rogers JA, Bowman TL, Jove R, Smithgall TE (1998) Activation of STAT3 by the c-Fes protein-tyrosine kinase. J Biol Chem 273:7072

10. Park WY, Ahn JH, Feldman RA, Seo JS (1998) c-Fes tyrosine kinase binds to and activates STAT3 after granulocyte- macrophage colony-stimulating factor stimulation. Cancer Lett 129:29

11. Senis Y, Zirngibl R, McVeigh J, Haman A, Hoang T, Greer PA (1999) Targeted disruption of the murine fps/fes proto-oncogene reveals that Fps/Fes kinase activity is dispensable for hematopoiesis. Mol Cell Biol 19:7436

12. Yu G, Smithgall TE, Glazer RI (1989) K562 leukemia cells transfected with the human c-fes gene acquire the ability to undergo myeloid differentiation. J Biol Chem 264:10276

13. Ferrari S, Manfredini R, Tagliafico E, Grande A, Barbieri D, Balestri R, Pizzanelli M, Zucchini P, Citro G, Zupi G, et al. (1994) Antiapoptotic effect of c-fes protooncogene during granulocytic differentiation. Leukemia 8 Suppl 1:S91

14. Ferrari S, Donelli A, Manfredini R, Sarti M, Roncaglia R, Tagliafico E, Rossi E, Torelli G, Torelli U (1990) Differential effects of c-myb and c-fes antisense oligodeoxynucleotides on granulocytic differentiation of human myeloid leukemia HL60 cells. Cell Growth Differ 1:543

15. Kim J, Feldman RA (2002) Activated Fes protein tyrosine kinase induces terminal macrophage differentiation of myeloid progenitors (U937 Cells) and activation of the transcription factor PU.1. Molecular and Cellular Biology 22:1903

16. Kim J, Ogata Y, Feldman RA (2003) Fes Tyrosine Kinase Promotes Survival and Terminal Granulocyte Differentiation of Factor-dependent Myeloid Progenitors (32D) and Activates Lineage-specific Transcription Factors. J Biol Chem 278:14978

17. Hackenmiller R, Kim J, Feldman RA, Simon MC (2000) Abnormal Stat activation, hematopoietic homeostasis, and innate immunity in c-fes-/- mice. Immunity 13:397

18. Zirngibl RA, Senis Y, Greer PA (2002) Enhanced endotoxin-sensitivity in Fps/Fes-null mice with minimal defects in hematopoietic homeostasis. Mol Cell Biol 22:2472

19. Senis YA, Craig AWB, Greer PA (2003) Fps/Fes and Fer protein-tyrosine kinases play redundant roles in regulating hematopoiesis. Experimental Hematology 31:1

20. Greer P, Haigh J, Mbamalu G, Khoo W, Bernstein A, Pawson T (1994) The Fps/Fes protein-tyrosine kinase promotes angiogenesis in transgenic mice. Mol Cell Biol 14:6755

21. Haigh J, McVeigh J, Greer P (1996) The fps/fes tyrosine kinase is expressed in myeloid, vascular endothelial, epithelial, and neuronal cells and is localized in the trans-golgi network. Cell Growth Differ 7:931

22. Bardelli A, Parsons DW, Silliman N, Ptak J, Szabo S, Saha S, Markowitz S, Willson JK, Parmigiani G, Kinzler KW, Vogelstein B, Velculescu VE (2003) Mutational analysis of the tyrosine kinome in colorectal cancers. Science 300:949

23. Yee SP, Mock D, Greer P, Maltby V, Rossant J, Bernstein A, Pawson T (1989) Lymphoid and mesenchymal tumors in transgenic mice expressing the v-fps protein-tyrosine kinase. Mol Cell Biol 9:5491

24. Yee SP, Mock D, Maltby V, Silver M, Rossant J, Bernstein A, Pawson T (1989) Cardiac and neurological abnormalities in v-fps transgenic mice. Proc Natl Acad Sci U S A 86:5873

25. Greer P, Maltby V, Rossant J, Bernstein A, Pawson T (1990) Myeloid expression of the human c-fps/fes proto-oncogene in transgenic mice. Mol Cell Biol 10:2521

26. Kim J, Ogata Y, Feldman RA (2003) Fes tyrosine kinase promotes survival and terminal granulocyte differentiation of factor-dependent myeloid progenitors (32D) and activates lineage-specific transcription factors. J Biol Chem

27. Keller P, Payne JL, Tremml G, Greer PA, Gaboli M, Pandolfi PP, Bessler M (2001) FES-Cre targets phosphatidylinositol glycan class A (PIGA) inactivation to hematopoietic stem cells in the bone marrow. J Exp Med 194:581

28. Senis YA, Sangrar W, Zirngibl RA, Craig AWB, Lee DH, Greer PA (2003) Fps/Fes and Fer Nonreceptor Protein-Tyrosine Kinases Regulate Collagen- and ADP-Induced Platelet Aggregation. Journal of Thrombosis and Haemostasis. In press

Figure Legends

Figure 1. Flow cytometry analysis of myeloid and B-cell precursors in bone marrow. (A, B) Bone marrow from *wt* (age = 2.9 ± 0.2 mo, *n* = 24) and *fps^{MF}* mice (age = 2.9 ± 0.2 mo, *n* = 22) was analyzed for levels of myeloid progenitors using markers for Ly6-G and CD11b. Statistically significant increases were present in undifferentiated granulocyte and monocyte progenitor populations (*a*; *p* = 0.015 and *b*; *p* = 0.024). (C, D) Analysis of B-cell precursors using markers for B220 and IgM revealed a statistically significant decrease in immature B-cell levels in *fps^{MF}* mice (age = 2.9 ± 0.2, *n* = 23, *c*; *p* = 0.02) compared to *wt* mice (age = 2.9 ± 0.2, *n* = 25).

Figure 2. Flow cytometry analysis of myeloid and B-cell precursors in spleen. (A, B) Levels of myeloid precursors in spleen suspensions from *wt* (age = 2.8 ± 0.04 mo, *n* = 8) and *fps^{MF}* (age = 2.8 ± 0.04 mo, *n* = 8) were determined using markers for Ly6-G and CD11b. The data show a statistically significant increase in single-positive CD11b undifferentiated progenitor populations in *fps^{MF}* mice (*a*: *p* = 0.003). (C, D) Immature B-cell levels in spleens of *wt* (age = 3.7 ± 0.4 mo, *n* = 9) and *fps^{MF}* (age = 3.7 ± 0.2 mo, *n* = 13) mice were assessed using markers for B220 and IgM. The data indicate that splenic B-cell precursor population levels are normal in *fps^{MF}* transgenic mice.

Figure 3. Colony forming unit assay. Bone marrow from *wt* and *fps^{MF}* siblings were grown in methylcellulose media containing two different cocktails of recombinant cytokines. (A) 50 ng/ml SF, 5 ng/ml IL-3, 10 ng/ml IL-6, 10 ng/ml Tpo. (B) 1 U/ml Epo and 5 ng/ml GM-CSF. Colonies were counted 8-days post plating and data are expressed as mean ± SEM. The results of three separate experiments indicate increases in the number of CFU-GM colonies with either

cocktail in fps^{MF} mice (p = 0.014 and p = 0.069 respectively). We also observed an increase in CFU-GEMM colonies in fps^{MF} mice with Epo and GM-CSF (p = 0.028).

Figure 4. T-cell maturation defects in secondary lymphoid organs of fps^{MF} mice. Flow analysis using markers for CD4 and CD8 were utilized to assess T-cell populations in the thymus and spleen. (A, B) Increased levels of CD4^{+}/CD8^{-} T-cell populations were observed in the thymus of fps^{MF} mice (3.7 ± 0.1 mo, n = 16, a; p < 0.006) relative to wt mice (age = 3.8 ± 0.2 mo, n = 12). (C, D) CD4^{+}/CD8^{-} and CD4^{-}/CD8^{+} populations in spleen were reduced in fps^{MF} mice (age = 3.7 ± 0.2 mo, n = 16, b; p < 0.006, c; p < 10^{-4}) in comparison to wt mice (age = 3.7 ± 0.2 mo, n = 12).

Figure 5. Enhanced STAT3/5 phosphorylation in fps^{MF} macrophages. Bone-marrow derived macrophages were stimulated with GM-CSF for 0-25 min, lysed and analyzed with phospho-specific antibodies to JAK2, STAT3 and STAT5. Antibodies to the latter proteins and to Fps and Fer were also used to assess mass levels of the respective proteins during the time course of the stimulation. Total protein content was measured by Sypro Ruby Protein fluorescent gel stain in order to confirm loading in each lane. The upper two panels represent the same blot at low and high exposures and depict the migration profiles of Fer, MFps and Fps. The data in the panels below show that JAK2 activation is unaffected and that STAT3/5 activation is enhanced in response to GM-CSF in fps^{MF} mice.

Figure 6. Effect of fps^{MF} on downstream effectors of GM-CSF signaling. Activation of the downstream signaling proteins p38 and pErk were assessed using phosphospecific antibodies. Mass levels were also assessed by corresponding control antibodies, and equal loading was confirmed by Sypro Ruby Protein fluorescent gel staining of total protein. The data show

increased kinetics of Erk activation in response to GM-CSF. No significant differences were observed in the kinetics of activation of p38 and of Akt and Jnk (data not shown).

Figure 7. Hypothetical model for Fps involvement in lineage commitment by hematopoietic progenitors. Increased mature circulating granulocytes and monocytes, and decreased lymphoid cells in fps^{MF} mice suggest a role for Fps at the level of the committed multi-lineage progenitor cell. Increased numbers of CFU-GEMM are also consistent with that role. Increased numbers of CFU-GM suggest this lineage-commitment role extends to the more mature bipotential granulomonocytic progenitor. The lack of a selective increase in monocytic or granulocytic cells argues against a lineage-determining role for Fps beyond this bipotential progenitor.

Figure 8. Molecular models supporting a role for Fps in activation of STAT3/5 downstream of GM-CSF. (A) ($fps^{+/+}$) In *wild-type* cells, Fps, JAK2 and LYN all participate in STAT3/5 phosphorylation. (B) ($fps^{KR/KR}$) In the presence of kinase-inactive Fps, there is some level of interference/competition that reduces the activation of STAT3/5 by JAK2 or LYN. (C) ($fps^{-/-}$) In the absence of Fps, there is no apparent effect on STAT3/5 activation, which presumably is mediated predominately by JAK2 and LYN. (D) (fps^{MF}) Membrane localization of myristoylated Fps (MFps) increases the effective localized concentration near the GM-CSFR β_c resulting in enhanced phosphorylation of STAT3/5.

Table 1. Peripheral blood analysis

White Blood Cells	*wild-type* (*n*)	*fps*[MF] (*n* / *p*-value)
White Blood Cells (10^9/L)	7.0± 0.4 (28)	**7.5 ± 0.7** (22 / 0.5)
Neutrophils (10^9/L)	1.3 ± 0.1 (27)	**1.7 ± 0.2** (21 / 0.02)
Neutrophils (%)	17.6 ± 1.2 (27)	**24.7 ± 1.8** (21 / <.001)
Lymphocytes (10^9/L)	5.6 ± 0.3 (27)	**5.3 ± 0.5** (21 / 0.6)
Lymphocytes (%)	80.9 ± 1.1 (27)	**72.7 ± 0.2** (22 / <0.001)
Monocytes (10^6/L)	47.6 ± 8.7 (28)	**152.4 ± 15.3** (21 / $<10^{-7}$)
Monocytes (%)	0.7 ± 0.1 (28)	**2.4 ± 0.3** (21 / $<10^{-6}$)
Basophils (10^6/L)	6.4 ± 0.9 (28)	**16.7 ± 1.9** (21 / $<10^{-5}$)
Basophils (%)	0.09 ± 0.01 (28)	**0.26 ± 0.04** (21 / 0.02)
Eosinophils (10^6/L)	undetectable (28)	undetectable (21 / ---)
Red Blood Cells (10^{12}/L)	9.1 ± 0.1 (28)	**7.8 ± 0.1** (22 / $< 10^{-10}$)

Blood was acquired from *wild-type* (4.5 ± 0.2 mo) and *fps*[MF] (4.3 ± 0.2 mo.) mice by cardiac puncture. Peripheral blood was analyzed using a SYSMEX XE-2100 Automated Hematological Analyzer. Data are presented as mean ± standard error of the mean (S.E.M.) along with P-values (*p*) and the number of animals used in the analyses (*n*). Statistically significant parameters are bolded.
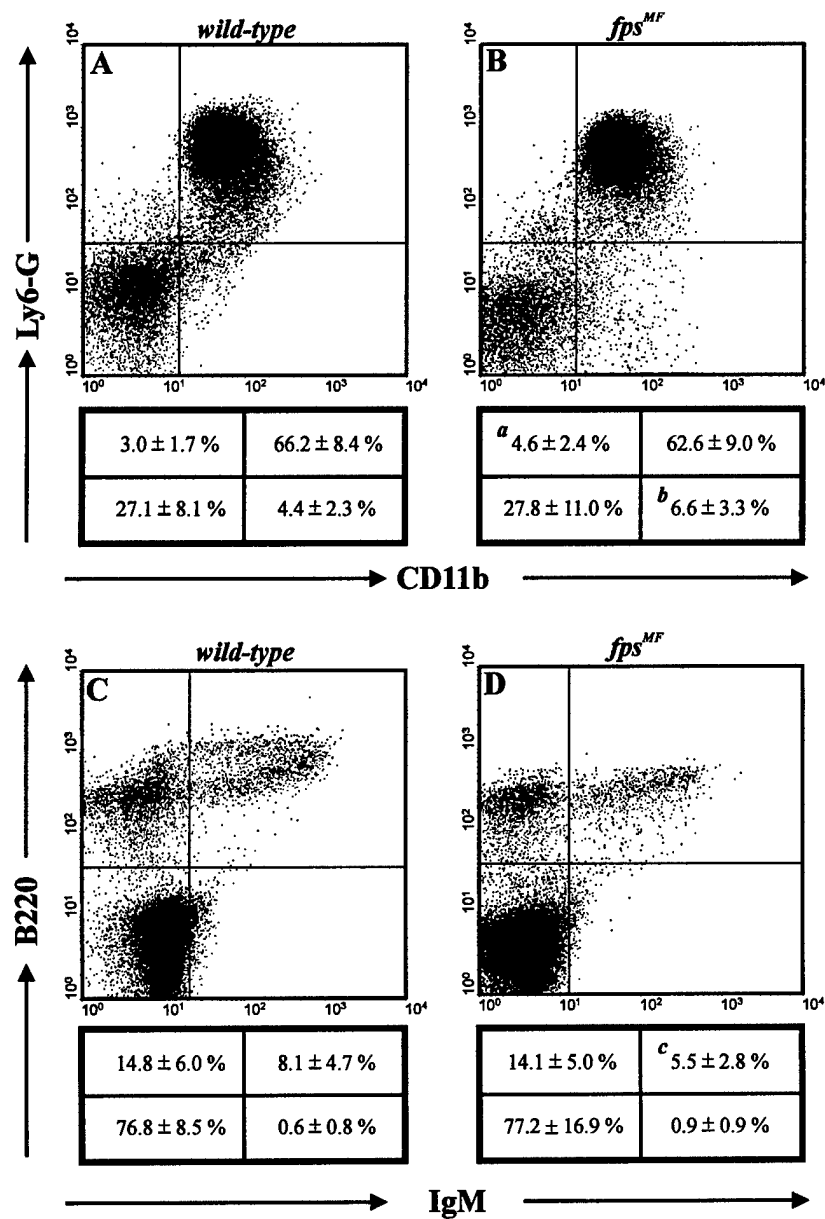
Figure 1

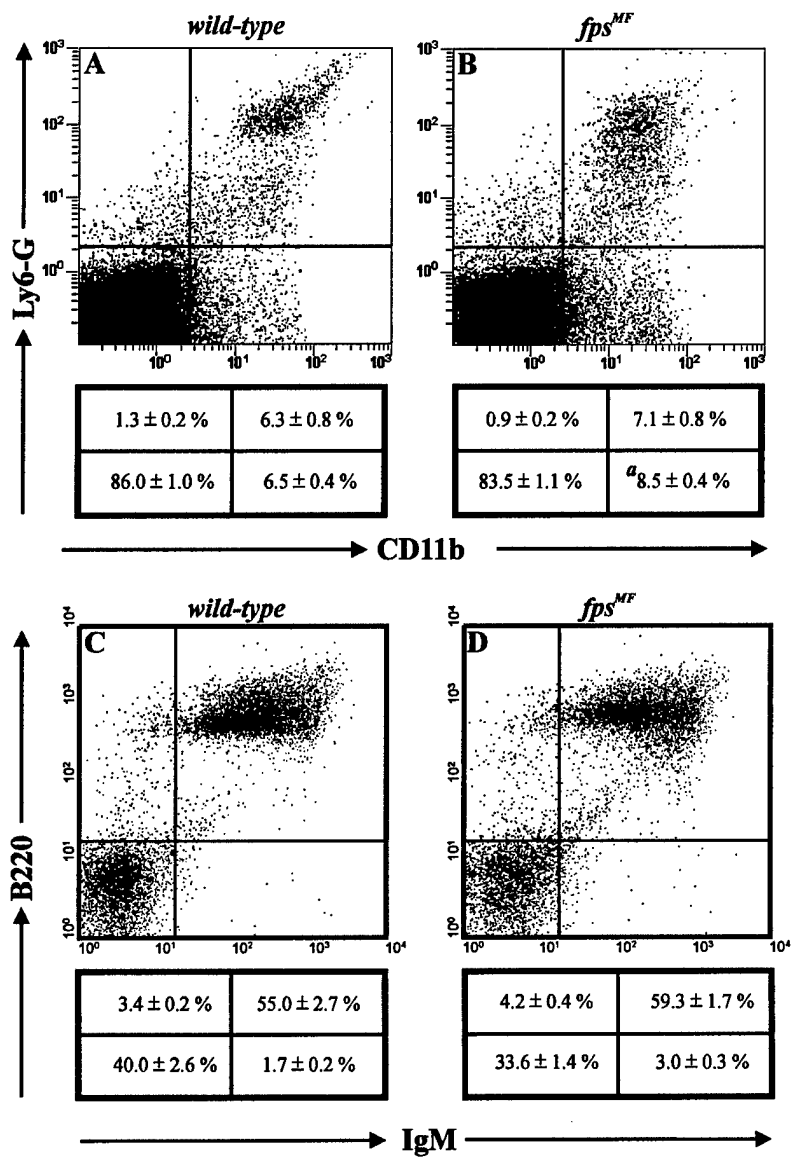A — wild-type — Ly6-G vs CD11b

| 3.0 ± 1.7 % | 66.2 ± 8.4 % |
| 27.1 ± 8.1 % | 4.4 ± 2.3 % |

B — fps^MF — Ly6-G vs CD11b

| [a] 4.6 ± 2.4 % | 62.6 ± 9.0 % |
| 27.8 ± 11.0 % | [b] 6.6 ± 3.3 % |

C — wild-type — B220 vs IgM

| 14.8 ± 6.0 % | 8.1 ± 4.7 % |
| 76.8 ± 8.5 % | 0.6 ± 0.8 % |

D — fps^MF — B220 vs IgM

| 14.1 ± 5.0 % | [c] 5.5 ± 2.8 % |
| 77.2 ± 16.9 % | 0.9 ± 0.9 % |

25

Figure 2

Figure 3

Figure 4

10.0 ± 1.3 %	75.4 ± 3.0 %	*wild-type* Thymus
7.1 ± 1.2 %	7.6 ± 0.9 %	

[a]16.1 ± 1.6 %	66.2 ± 2.8 %	*fps*[MF] Thymus
8.4 ± 0.8 %	9.4 ± 0.7 %	

22.1 ± 1.2 %	0.8 ± 0.1 %
69.2 ± 1.7 %	8.0 ± 0.6 %

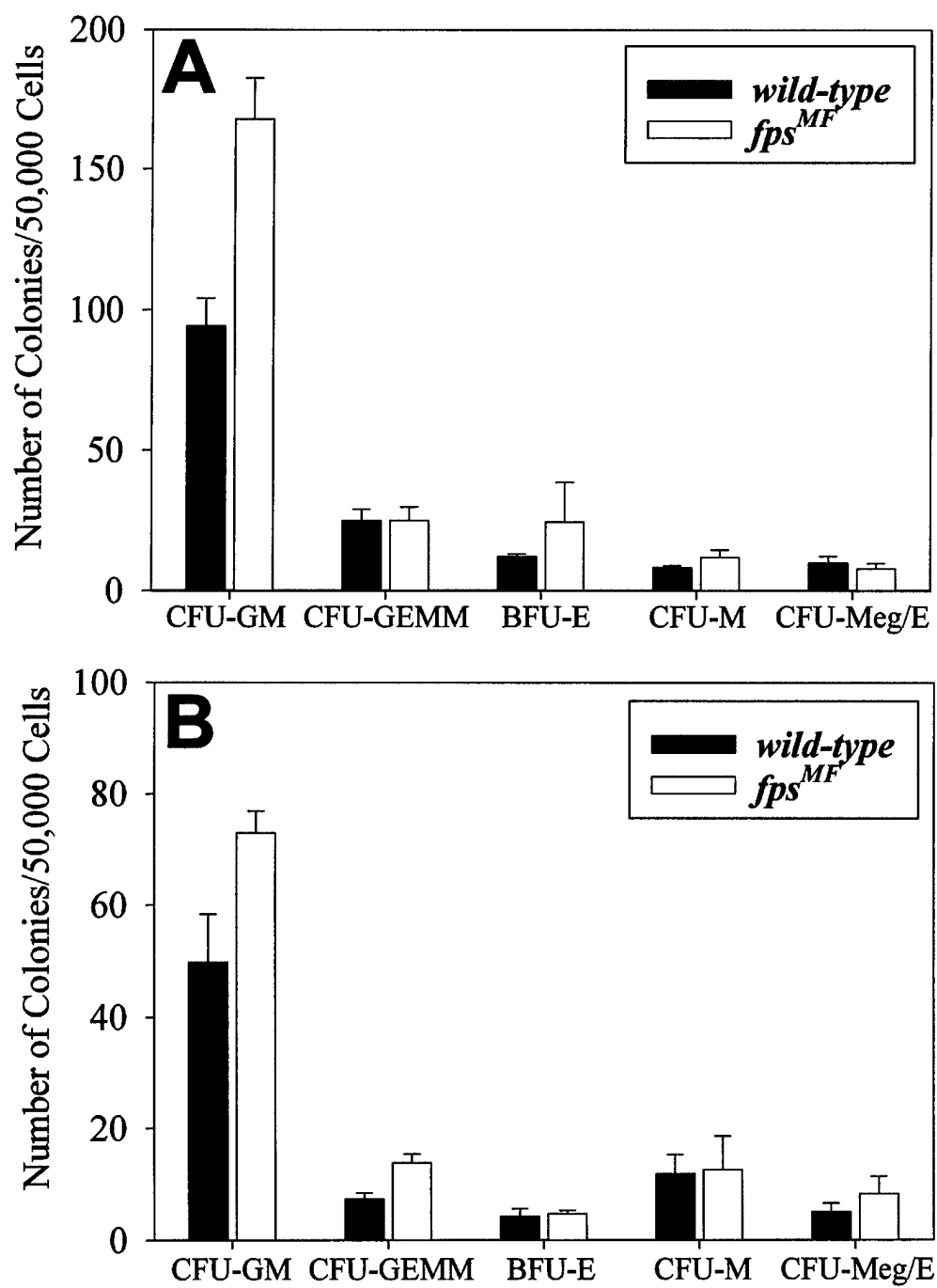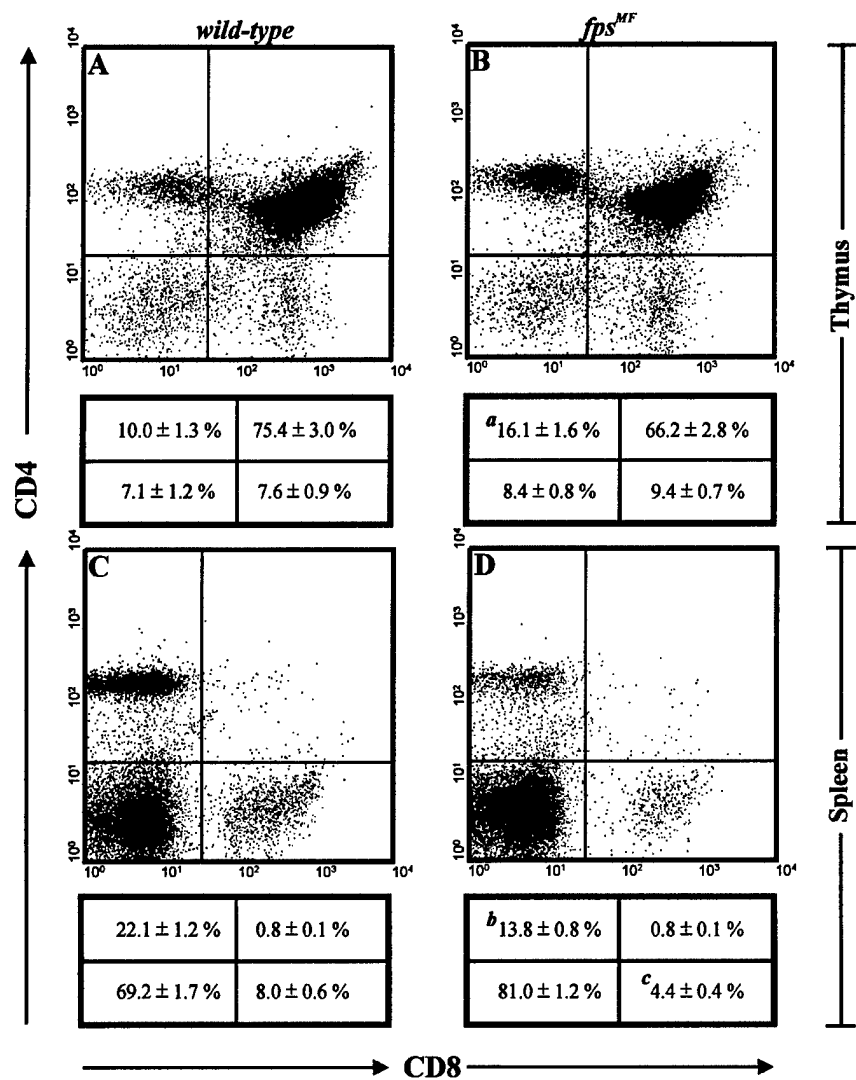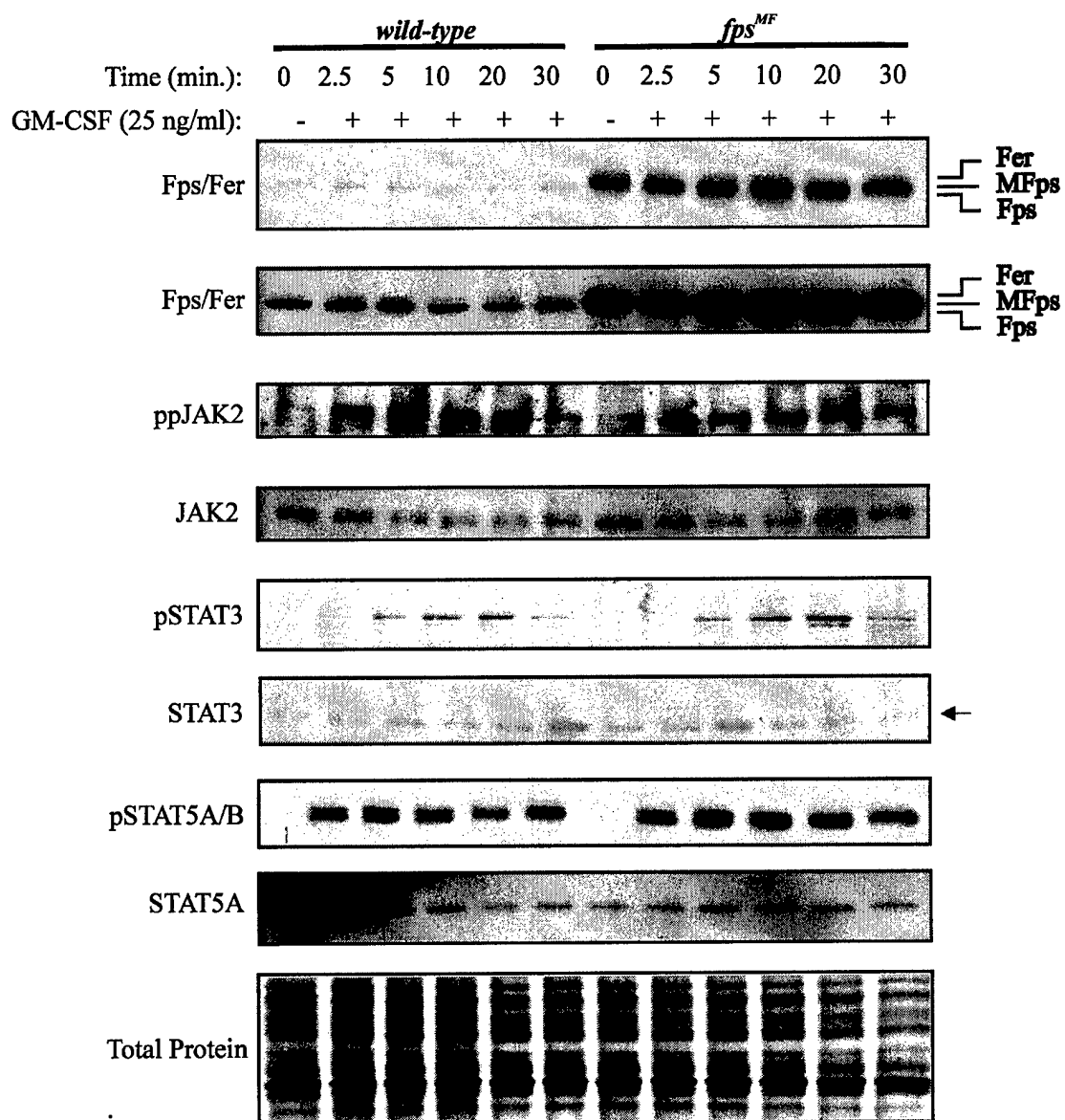|	
[b]13.8 ± 0.8 %	0.8 ± 0.1 %
81.0 ± 1.2 %	[c]4.4 ± 0.4 %

CD4

CD8

Thymus

Spleen

Figure 5

Figure 6

Figure 7

Figure 8

A *fps*$^{+/+}$

GM-CSFR

α β$_c$

Fps Jak2

STAT3/5 LYN

P

Dimerization and
transcriptional activation

B *fps*$^{KR/KR}$

GM-CSFR

α β$_c$

Fps Jak2

STAT3/5 LYN

P

Dimerization and
transcriptional activation

C *fps*$^{-/-}$

GM-CSFR

α β$_c$

Jak2

STAT3/5 LYN

P

Dimerization and
transcriptional activation

D *fps*^{MF}

GM-CSFR

α β$_c$

Fps Jak2

MFps STAT3/5 LYN

P

Dimerization and
transcriptional activation

32